ELSEVIER

Agricultural and Forest Meteorology 113 (2002) 159–183

AGRICULTURAL AND FOREST METEOROLOGY

www.elsevier.com/locate/agrformet

Footprint modeling for vegetation atmosphere exchange studies: a review and perspective

Hans Peter Schmid*

Department of Geography, Indiana University, 47405 Bloomington, IN 47405, USA

Accepted 3 April 2002

Abstract

The footprint of a turbulent flux measurement defines its spatial context. With the onset of long-term flux measurement sites over forests and other inherently inhomogeneous areas, and the development of the FLUXNET program, the need for flux footprint estimations has grown dramatically. This paper provides an overview of existing footprint modeling approaches in the critical light of hindsight and discusses their respective strengths and weaknesses. The second main objective of this paper is to establish a formal connection between micrometeorological measurements of scalar fluxes and their mass conservation equation, in a surface–vegetation–atmosphere volume. An important focus is to identify the limitations of the footprint concept and to point out situations where the application of footprint models may lead to erroneous conclusions, as much as to demonstrate its utility and power where warranted. Finally, a perspective on the current state-of-the-art of footprint modeling is offered, with a list of challenges and suggestions for future directions.

Keywords: Footprint; Micrometeorology; Vegetation atmosphere exchange; Modeling; Flux measurements

1. Introduction

Why do we need footprint models? The footprint of a turbulent flux measurement defines the spatial context of the measurement. It is something akin to the "field of view" of the measurement of surface atmosphere exchange. When turbulent flux sensors are deployed, the objective is usually to measure signals that reflect the influence of the underlying surface on the turbulent exchange. Over a homogeneous surface, the exact location of a sensor is not an issue, because the fluxes from all parts of the surface are by definition equal. However, if the surface is inhomogeneous, the measured signal depends on which part of the surface has the strongest influence on the sensor, and thus on the location and size of its footprint.

The growing importance of observational issues over inhomogeneous terrain is illustrated by the number of publications per year relating to the footprint concept. Since 1972, when Pasquill's original paper on the *effective fetch* was published, these have been increasing exponentially with a doubling period of about 3–4 years. This development is in parallel with a shift of focus of micrometeorology from "ideal" homogeneous sites to inhomogeneous areas of naturally variable land cover and urban areas. Over inhomogeneous sites, the horizontal and vertical variability of measured fluxes of surface–atmosphere exchange must be accounted for, and the question of spatial

* Tel.: +1-812-855-6303; fax: +1-812-855-1661.
E-mail address: hschmid@indiana.edu (H.P. Schmid).

0168-1923/02/$ – see front matter
PII: S0168-1923(02)00107-7

representativeness of flux measurements arises. In the face of these growing concerns, the footprint concept provides a quantitative tool to establish the spatial frame of reference of surface–atmosphere exchange measurements. Here, the term *footprint* is used to summarize the notions of effective fetch, source area or sensor footprints, but each of these terms will be defined more formally, below.

In Section 2, the development history of the footprint concept is outlined briefly, starting with notions of fetch and internal boundary layers. This is followed by an overview of different existing flux footprint modeling approaches and their respective strengths and weaknesses. Specific applications of footprint models are mentioned where the context demands this, but a detailed review of footprint applications is beyond the purpose of this paper.

The second main objective of this paper is to review the theoretical foundations of the footprint concept in a critical light, by establishing a formal connection between micrometeorological measurements of fluxes or concentrations of trace gases above a vegetation canopy and their mass conservation equation, in a surface–vegetation–atmosphere volume (Section 3). An important focus is to identify the limitations of the footprint concept and to point out situations where the application of footprint models may lead to erroneous conclusions, as much as to demonstrate its utility and power were warranted.

Finally, a perspective on the future requirements and potential of the flux footprint approach is offered in Section 4, closing with a summary of problems, challenges, and potential research questions in flux footprint modeling.

2. Concept and model approaches of the flux footprint and its variants

The footprint of a measurement is the transfer function between the measured value and the set of forcings on the surface–atmosphere interface. Formally, this notion is expressed in an integral equation, following Pasquill and Smith (1983):

$$\eta(\mathbf{r}) = \int_{\Re} Q_\eta(\mathbf{r}+\mathbf{r}')\, f(\mathbf{r}, \mathbf{r}')\, \mathrm{d}\mathbf{r}' \qquad (1)$$

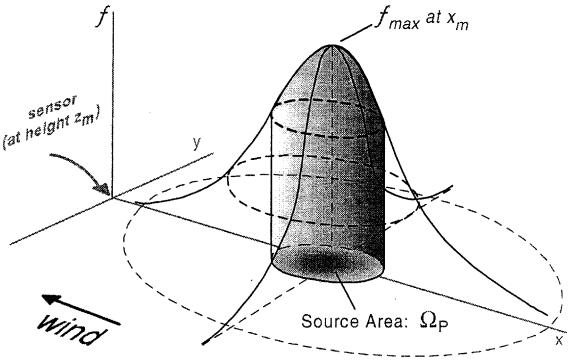

Fig. 1. Schematic of the source weight function, or footprint function. The source weight is small for small separation distances. It rises to a maximum with increasing distance and then falls off again to all sides as the separation is further increased (adapted from Schmid, 1994).

where η is the measured value at location $\mathbf{r}$, $Q_\eta(\mathbf{r}+\mathbf{r}')$ the distribution of source or sink strength in the surface–vegetation volume, and $f(\mathbf{r}, \mathbf{r}')$ is the footprint or transfer function, depending on $\mathbf{r}$, and on the separation between measurement and forcing, $\mathbf{r}'$. The integration is performed over a domain $\Re$. Fig. 1 is a schematic representation of the footprint function and its relation to a sensor at height above the surface. In contrast to radiation footprints (Schmid, 1997), the turbulent transport footprint is not symmetric about the vertical axis of the sensor. Generally, the value of the footprint function or source weight, f, rises to a maximum at some distance upstream and falls off smoothly to all sides. The integral beneath the footprint function expresses the total surface influence on the signal measured by the sensor.

This general relation defines the footprint and, with some limitations, is common to all sensor footprints or related concepts. Differences exist in the type of measured quantity, η (e.g., scalar flux, bulk gradient, Bowen ratio, or scalar concentration over a given background), in the approach to estimate the transfer function, f (e.g., Eulerian analytical or numerical, or Lagrangian stochastic (LS) simulation), in the degree of symmetry and homogeneity assumed in the flow in which f is embedded, and in the specification of the integration domain, $\Re$. In the following, various approaches and variants to the footprint concept are discussed by outlining its development history.

2.1. Internal boundary layers and Pasquill's effective fetch

In the pre-history of the footprint concept are considerations of internal boundary layer growth, in response to flow across a step-change in the thermal or mechanical surface forcing, going back to the original study by Elliott (1958). Garratt (1990) provides a comprehensive review of internal boundary layer work. In the case of a discrete crosswind discontinuity, the degree of readjustment to new conditions can be described by various boundary layer interfaces of growing depth with distance downwind of the surface transition, based on a balance of horizontal advection and vertical turbulent diffusion. One such interface marks the initial modification of the concentration, flux, or flow field by the downstream surface. The height of this initial modification interface (IMIF) is defined as the height, up to which the flow conditions deviate from the upstream equilibrium by more than a small arbitrary factor (e.g., Peterson, 1969). The height to which the flow is in equilibrium with the downstream surface (the equilibrium interface, EIF) is assumed about 10% of the IMIF height (Peterson, 1969; Perrier and Tuzet, 1991). Elliott (1958) and Schlichting (1968) found that the depth of these interfacial layers in neutral conditions grow with distance from the surface transition in a 4/5 power law relationship. Despite efforts by Panofsky (1973), Rao (1975), and Højstrup (1981), among others, to enhance the physical basis of internal boundary layer growth estimates, the 4/5 power relation between fetch and height was commonly used, and even simplified into an approximate 1/100 height to fetch ratio as a rule-of-thumb for measurements downwind of surface discontinuities (Garratt, 1990). Due to its simplicity, the use of this rule-of-thumb remained widespread, although it was shown to be inadequate and outdated (Leclerc and Thurtell, 1990).

Simple fetch estimates and the internal boundary layer approach become unsuitable, if the problem of surface inhomogeneity is extended to two-dimensional surface patchiness, rather than a one-dimensional crosswind discontinuity. This problem was first addressed by Pasquill (1972), who suggested an analogy between the developing zone of influence downwind from a surface element, and a diffusing plume of a scalar emitted at that surface element. Pasquill (1972) developed his analysis for a "momentum plume", where the surface elements appear as individual sinks. He postulated that, regarding a particular elementary area in isolation, the momentum deficit that this sink produces at a given height rises to a maximum at a distance downwind and then falls off continuously as distance is further increased. If the momentum deficit plume can be geometrically inverted, it is identical to the distribution of the influence that each elemental surface momentum sink exerts on the momentum deficit at a given reference location above the surface. Pasquill's assumption of Gaussian diffusion in both vertical and lateral direction, allowed him to adopt Smith's (1957) reciprocal relation for ground and elevated sources to achieve the plume inversion. He concluded that the functional form of the "momentum deficit distribution" is precisely that contained in the theoretical ground-level concentration distribution from an elevated scalar diffusion source.

Although this is not formally presented in this way by Pasquill (1972), his rationale follows the integral transfer function approach of (1). His inverted "momentum deficit distribution" implies the idea of a footprint transfer function for momentum, and he used the "momentum sink"–"scalar source" analogy to estimate the footprint by a Gaussian diffusion model. Pasquill (1972) defined a surface area of influence, which he termed the *effective fetch*, bounded by a concentration isopleth of the plume, with the arbitrary value of half of the maximum concentration. The dimensions of this approximately elliptical effective fetch region, relative to a sensor location, depend on the sensor height, the surface roughness, and atmospheric stability. Pasquill's effective fetch estimates are the first attempt documented in the literature, to account for the spatial context of measurements of some aspect of turbulent exchange over a surface with two-dimensional irregular patchiness.

2.2. The inverted plume assumption

Although Pasquill (1972) obviously considered a flow field that is perturbed by the surface patchiness, the inverted plume assumption contains an inherent contradiction, because it implicitly requires that the surface roughness and stability are uniform in the region. As will be seen, the majority of current footprint models rely implicitly or explicitly on some form of

the inverted plume assumption. Accordingly, careful considerations of its ramifications are warranted here.

In terms of (1), the inverted plume approach assumes that the footprint function, f, is only dependent on the separation vector between source and sensor, $\mathbf{r}'$, and not on the location, $\mathbf{r}$, itself, so that it is postulated that

$$f(\mathbf{r}, \mathbf{r}') \approx f(\mathbf{r}') \tag{2}$$

A consequence of (2) is that $f(\mathbf{r}')$ must also be independent of Q_η in (1). If there is a spatially variable forcing Q_η that affects not only $\eta(\mathbf{r})$, but also the turbulence field, and thus f, the inverted plume approach is fundamentally flawed. This is obviously the case for the distribution of momentum sinks, as in Pasquill (1972), or spatial variations in buoyancy production within the integration domain, $\mathfrak{R}$, of (1). However, if individual surface elements are of a length scale λ, and the sensor height, for which a footprint is evaluated, is $z_\mathrm{m} \gg \lambda$, it may be assumed that turbulent mixing and the integral in (1) cancel individual spatial perturbations in f. In this case, the constraint (2) takes the form of a linearization or small-perturbation approximation by requiring that f be dependent only on the spatial integral of the dynamically active surface forcings, and not on its spatial perturbations. Alternately, if f is decomposed into a spatial average $\langle f \rangle$ and perturbations f'', then

$$\eta(\mathbf{r}) = \int_{\mathfrak{R}} Q_\eta(\mathbf{r}+\mathbf{r}')\langle f\rangle(\mathbf{r}')\,\mathrm{d}\mathbf{r}' + \int_{\mathfrak{R}} Q_\eta(\mathbf{r}+\mathbf{r}') f''(\mathbf{r}')\,\mathrm{d}\mathbf{r}' \tag{3}$$

and the inverted plume assumption requires that

$$\int_{\mathfrak{R}} Q_\eta(\mathbf{r}+\mathbf{r}')\langle f\rangle(\mathbf{r}')\,\mathrm{d}\mathbf{r}' \gg \int_{\mathfrak{R}} Q_\eta(\mathbf{r}+\mathbf{r}') f''(\mathbf{r}')\,\mathrm{d}\mathbf{r}' \tag{4}$$

Some aspects of spatial averages over inhomogeneous areas are revisited in Section 3.

In summary, the inverted plume assumption is seen to be valid in areas where the spatial inhomogeneities are primarily due to variations in the source or sink strength of passive scalars, and any variations in mechanical or thermal turbulence production are confined to small length scales, compared to the reference height of footprint considerations.

2.3. The cumulative effective fetch of Gash (1986)

Gash (1986) adopted Pasquill's (1972) idea to view an area of heterogeneous surface fluxes as an array of elemental sources in a two-dimensional flow approach. He estimated the effect of a limited fetch for evaporation measurements by considering an upwind array of spanwise elemental line sources, each occupying an infinitesimal strip of width δx. For a sensor mounted at a height z_m, water vapor diffusing from a distance x is on average sensed with a concentration $\rho_v(x, z_\mathrm{m})$. To obtain an equation for this concentration, Gash (1986) applied an analytical solution by Calder (1952) to the basic advection-diffusion equation, assuming neutral stratification and a uniform wind velocity that is independent of height, U. After differentiation with respect to z_m and integration with respect to x, from zero to a distance x_L, he obtained an equation for the vertical concentration gradient at z_m as caused by the evaporation (E) from a (uniform) strip of streamwise dimension x_L

$$\frac{\partial \rho_v(z_\mathrm{m})}{\partial z_\mathrm{m}} = -\frac{E}{k u_* z_\mathrm{m}} \exp\left[-\frac{U z_\mathrm{m}}{k u_* x_L}\right] \tag{5}$$

where k is von Kàrmàn's constant. With a uniform eddy diffusivity, $K(z_\mathrm{m}) = k u_* z_\mathrm{m}$, the gradient at z_m is proportional to the turbulent flux due to sources on the strip x_L. As x_L approaches infinity, (5) takes the form of the familiar surface layer flux–gradient relation for homogeneous and neutral conditions with unlimited fetch. Taking the ratio of the flux due to x_L to the homogeneous flux ($x_L = \infty$) as F, leads to the definition of x_F as the "F-fraction effective fetch"

$$x_F = -\frac{U z_\mathrm{m}}{k u_* \ln(F)} \tag{6}$$

(Gash (1986) expressed F in percent, so that the argument in the logarithm of (6) becomes $F/100$).

In (6), F is an integral footprint function that expresses the upstream-integrated source weight as the portion of a measured flux contributed by sources within a limited fetch, scaled by the total flux from sources in an unlimited fetch (Fig. 2a). Gash (1986) did not discuss a differential footprint function as defined by (1), but, as pointed out by Schuepp et al. (1990), the corresponding $f(x) = \mathrm{d}F/\mathrm{d}x$ for

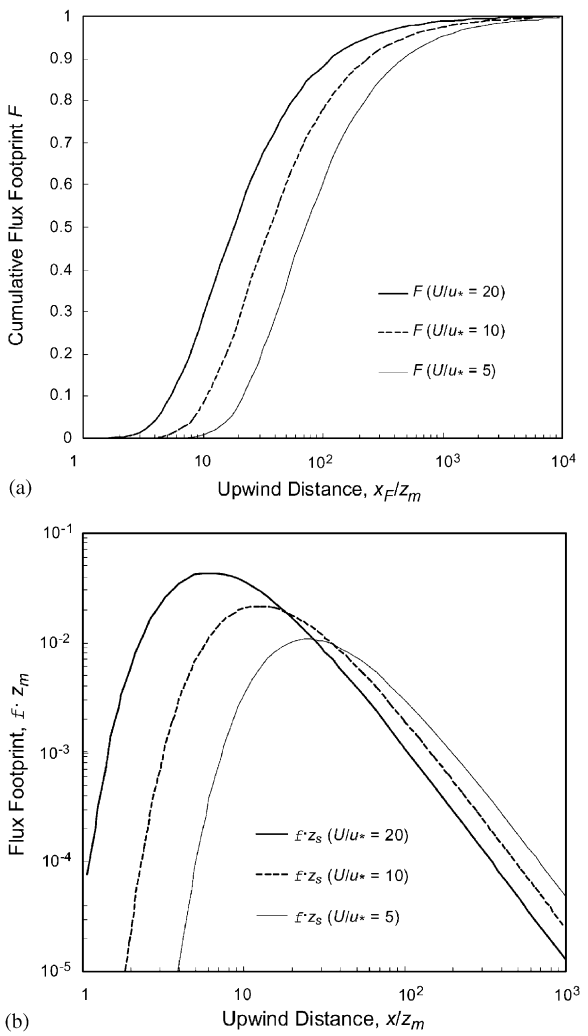

Fig. 2. (a) Cumulative flux footprint curves for the analytical model of Gash (1986) and Schuepp et al. (1990). The shape of the curves is similar to those of other models. Thus, they are shown here as illustrative examples. (b) Same as (a), but for the differential footprint. The shape of the curves is similar to those of other models. Thus, they are shown here as illustrative examples.

two-dimensional flow follows from (6) as

$$f(x) = \frac{Uz_\mathrm{m}}{ku_*x^2}\exp\left[-\frac{Uz_\mathrm{m}}{ku_*x}\right] \tag{7}$$

Clearly, this flux footprint relationship (Fig. 2b) is derived using crude and unrealistic assumptions, but its overall characteristics are the same as those of more sophisticated modern footprint models. In this sense, Gash (1986) is the first study that refers to a form of flux footprint in the way the term is used today in micrometeorology.

2.4. The source area of Schmid and Oke (1988, 1990)

Similar to Pasquill's (1972) original approach, Schmid (1988) and Schmid and Oke (1988, 1990) (henceforth, SO88/90) used the concentration distribution from a continuous point source of a passive scalar to approximate the footprint function for a sensor mounted at height. The footprint or source weight distribution function provides information about the relative weights of individual point sources. However, from an experimental perspective it is significant to obtain an estimate of what region of the surface is most effectively influencing the measured signal. SO88/90 considered the smallest possible area to be responsible for a given relative weight, P, (half, say $P = 0.5$) to the measured value and termed it the *source area* of level P. They showed that this source area, Ω_P, is bounded by a footprint isopleth $f(x', y', z_\mathrm{m}) = f_P$ (see Fig. 1), such that P is the fraction of the total integrated footprint function, φ_tot, contained in the source area

$$P = \frac{\varphi_P}{\varphi_\mathrm{tot}} = \frac{\displaystyle\iint_{\Omega_P} f(x', y', z_\mathrm{m})\,\mathrm{d}x'\,\mathrm{d}y'}{\displaystyle\int_{-\infty}^{+\infty}\int_{-\infty}^{+\infty} f(x', y', z_\mathrm{m})\,\mathrm{d}x'\,\mathrm{d}y'} \tag{8}$$

where φ_P is the integral of the footprint over the source area, Ω_P. The source area approach combines elements of both Pasquill's (1972) and Gash's (1986) earlier work: it considers a two-dimensional area bounded by a footprint function isopleth (like Pasquill, 1972), but in contrast to Pasquill (1972) the bounding isopleth is defined by the fraction of the integrated footprint contained in it, similar to Gash's (1986) cumulative footprint.

To obtain an estimate for $f(x', y', z_\mathrm{m})$, SO88/90 used the plume diffusion model by Gryning et al. (1987). In contrast to the earlier footprint work, this model takes account of the non-Gaussian diffusion in the vertical, and the shape of the profile is expressed in terms of Monin–Obukhov (M–O) similarity theory. Using van Ulden's (1978) analytical solution to the

advection-diffusion equation, it assumes self-similar profiles of wind velocity and eddy diffusivity expressed by power laws that are subsequently matched to M–O similarity surface-layer profiles (Gryning et al., 1987). Like Pasquill (1972), SO88/90 approximated the footprint function by the three-dimensional concentration distribution. Thus, their footprint and source area estimates are valid only for measurements of scalar concentrations, but not fluxes (Horst and Weil, 1992; Schmid, 1994). To address this problem Schmid (1994) adapted the analytical flux footprint expression of Horst and Weil (1992) to obtain a source area model for passive scalar fluxes, and to expand the range of stability over which it can be applied. It turns out that the flux source areas are smaller than the concentration source areas, but show very similar dependence on measurement height and stability (see also Wilson and Swaters, 1991).

The location of the bounding isopleth for the P-level source area, $f(x', y', z_m) = f_P$, cannot be expressed explicitly as $y' = f^{-1}(x'|f = f_P)$. The dimensions of the isopleth need to be determined numerically. To facilitate the use of their source area model, Schmid and Oke (1990), and Schmid (1994) presented parameterization formulae for the principal source area dimensions as functions of measurement height, stability, and crosswind turbulence. While these formulae are very easy to use, they are valid only over a limited interval of heights and stability.

Using the source area models of SO88/90, Schmid et al. (1991) provided the first experimental evidence that the footprint approach expresses the spatial representativeness of turbulent flux measurements over inhomogeneous areas. They showed that the median of the difference in heat flux, measured by two spatially separated sensors, reduces with increasing source area size (see their Fig. 9). With a larger source area, the sensor is implicitly averaging over a larger area, and the measurement becomes more spatially representative.

2.5. Eulerian analytic flux footprint models

The term *flux footprint* was coined by Schuepp et al. (1990). This study was also the first to present a differential footprint model, as defined by (1), for the flux of a passive scalar under neutral conditions. They explored several approaches to the advection-diffusion equation, and then pursued the approximate solution by Calder (1952) further, as proposed by Gash (1986). They found good qualitative agreement between aircraft measurements of CO_2 flux profiles across an isolated flat island and predictions by the equivalent of (7). A comparison with footprint calculations based on Lagrangian simulations of particle trajectories by Leclerc and Thurtell (1990) points to two important weaknesses of Calder's solution: first, the constant U/u_* in (7), and second, the limitation to neutral stability.

Both of these limitations were overcome by the footprint model of Horst and Weil (1992). They extended the results of Schuepp et al. (1990) with a more realistic analytic dispersion model that accounts for the effects of atmospheric stability and the variations of wind speed with height within the limits of the surface layer scaling regime (Holtslag and Nieuwstadt, 1986). The original Horst and Weil model (henceforth, the HW-model) was further developed in a series of papers (Horst and Weil, 1994, 1995; Finn et al., 1996). The currently recommended version of the HW-model is summarized in Horst (1999).

Horst and Weil (1992) showed that the dependence of the flux footprint on crosswind location is proportional to the crosswind concentration distribution for a unit surface point source. Like SO88/90 in their source area model, Horst and Weil (1992) used an approximate vertical concentration profile equation proposed by van Ulden (1978) and Horst (1979) to formulate the crosswind integrated flux footprint, $\bar{f}^y$:

$$\bar{f}^y(x, z_m) = -\int_{z_0}^{z_m} \bar{u}(z) \frac{\partial}{\partial x} \bar{C}^y(x, z)\, dz \tag{9}$$

where the crosswind integrated concentration, $\bar{C}^y$ was given by van Ulden (1978) as

$$\bar{C}^y(x, z) = \frac{A}{U\bar{z}} \exp\left\{-\left(\frac{z}{b\bar{z}}\right)^r\right\} \tag{10}$$

Here, A and b are given as functions of the exponent (or shape parameter), r. Gryning et al. (1983) provided an approximate formula for r in terms of the mass-weighted mean plume height, $\bar{z}(x)$, and stability. U is the mass-weighted mean plume velocity. Although van Ulden's solution is analytic, it is

implicit in x by

$$\bar{z}(x) = \frac{\int_0^\infty z\bar{C}^y(x,z)\,\mathrm{d}z}{\int_0^\infty z\bar{C}^y(x,z)\,\mathrm{d}z} \tag{11}$$

Using K-theory, van Ulden (1978) expressed the growth rate of $\bar{z}(x)$ as

$$\frac{\mathrm{d}\bar{z}}{\mathrm{d}x} = \frac{K(p\bar{z})}{\bar{u}(p\bar{z})p\bar{z}} \tag{12}$$

where K is the eddy diffusivity, and p is a (weak) function of r.

Approximate (implicit) formulae for both U and $\mathrm{d}\bar{z}/\mathrm{d}x$, in terms of M–O similarity relations, were given by Gryning et al. (1983, 1987). Horst and Weil (1994, 1995) provided an exact analytical solution for $x(\bar{z})$ that needs to be inverted numerically. Thus, although the HW-model is expressed by analytic formulae, it can only be evaluated numerically.

Horst and Weil (1992) presented a normalized crosswind integrated footprint, F, which strongly depends on $\bar{z}/z_\mathrm{m}$, and exhibits only very weak remaining dependence on stability and surface roughness, because these dependences are already accounted for by $\bar{z}/z_\mathrm{m}$

$$\Phi = \frac{z_\mathrm{m}\bar{f}^y(x,z_\mathrm{m})}{\mathrm{d}\bar{z}/\mathrm{d}x} \tag{13}$$

They demonstrated this universality by a comparison with an LS footprint model. To address the problem that their model can only be evaluated numerically, Horst and Weil (1994) provided an approximate analytical expression, which is exact for power law wind profiles (Horst, 1999)

$$\Phi \approx A\left[\frac{z_\mathrm{m}}{\bar{z}}\right]^2 \frac{\bar{u}(z_\mathrm{m})}{U(\bar{z})}\exp\left\{-\left[\frac{z_\mathrm{m}}{b\bar{z}}\right]^r\right\} \tag{14}$$

The analytic model of Horst and Weil (1992) and its successors have been widely used since their publication. The same theoretical framework was used in the flux and concentration source area models by Schmid (1994, 1997) and was used in the analysis of Stannard (1997), to determine the fetch requirements of Bowen ratio measurements. Horst (1999) used it to formulate equivalent flux footprint estimates for fluxes measured by the bulk profile technique, and to generalize the findings of Stannard (1997) about Bowen ratio footprints.

In a critique of the HW-model, Haenel and Grünhage (1999) pointed out that the implementation of (14) as suggested by Horst (1999) causes Φ to overshoot its theoretical asymptotic constraint of unity at large $\bar{z}(x)$. They offered an alternative model that identically complies to the constraint. However, as discussed below, this objective of mathematical exactness is reached only at the expense of physical content.

Haenel and Grünhage (1999) attributed the faulty asymptotic behavior of (14) to the use of M–O similarity profiles in the formulation for the shape factor, r, suggested by Gryning et al. (1983, 1987), instead of power law profiles. van Ulden's (1978) solution to obtain the concentration distribution from a unit surface point source (10), is based on the use of power laws for wind speed ($\bar{u} = \alpha_u z^m$) and eddy diffusivity ($K = \alpha_K z^n$), where α_u and α_K are proportionality constants to be determined empirically. Despite the lack of a physical basis for these power laws, their use is pragmatically justified by their mathematical simplicity, which allows analytical solutions. The shape parameter, r, in (10) is related to the exponents of these power laws as $r = 2 + m – n$ (van Ulden, 1978). However, to introduce similarity theory into the solution (10), Gryning et al. (1983, 1987) suggested to fit power laws to the M–O similarity profiles, to determine the dependence of r on $\bar{z}/L$ (where L is the Obukhov length), and thus indirectly on x through $\bar{z}(x)$. Thus, Haenel and Grünhage (1999) noted that the M–O representation of r gains physical meaning at the expense of some of its original consistency with the profiles of wind speed and eddy diffusivity that are assumed to be independent of x, but Horst (2001) pointed out that the profiles are still locally independent of x. Horst (2001) further asserted that the departure of the HW-model from its theoretical constraint is due to the introduction of analytical simplifications to the Horst and Weil (1992) expressions, and is not a consequence of following Gryning et al. (1983, 1987) for r.

Nevertheless, to address the problem of the asymptotic limit, Haenel and Grünhage (1999) proposed to remain in the "power law world" longer in their derivation of an analytical form of (9) and prescribed r to be independent of $\bar{z}$ and thus x. Thus, r is a constant in (10), and it becomes possible to integrate (9) analytically (Haenel and Grünhage, 1999), as expressed

in normalized form by

$$\Phi = AB\left[\frac{z_m}{\bar{z}}\right]^{(3+r)/2} \exp\left\{-\left[\frac{z_m}{b\bar{z}}\right]^r\right\} \quad (15)$$

where B is an analytical function of r (see Eq. (23) in Haenel and Grünhage, 1999). Applying Schmitt's conjugate powers for the power laws of wind speed and diffusivity ($m + n = 1$), they finally reintroduced M–O theory at this stage by expressing m and thus r as a function of stability z_m/L and measurement height, z_m/z_0, where z_0 is the surface roughness length. Incidentally, (15) is a special case of (14) for conjugate power laws in the specification of $U(\bar{z})$ (Horst, 2001).

To recover the non-normalized flux footprint, $\bar{f}^y$, from Φ in (14) or (15), or to express Φ in terms of the streamwise distance, x, rather than $\bar{z}$, a practical relation for $d\bar{z}/dx$, such as (12), is needed (see (13)). Both the HW-model and Haenel and Grünhage (1999) follow van Ulden (1978) here, and use M–O similarity profiles for K and $\bar{u}$, and ignore the weak dependence of p on r. The result is an implicit similarity relation for $d\bar{z}/dx$ that can only be solved for $\bar{z}$ numerically.

By remaining in the "power law world" even for the evaluation of (12), Kormann and Meixner (2001) avoided this problem. They continue using the power law profiles for K and $\bar{u}$ in (12) and were thus able to integrate it analytically. The resulting explicit equation for $\bar{z}$ allows the determination of the mean plume velocity U, which leads to an alternative form of the crosswind integrated concentration distribution (10) first proposed by Lin and Hildemann (1996) that is explicit in x and z. Using K-theory and the power law profile for K, the crosswind integrated footprint follows directly as (compare Eqs. (17)–(21) in Kormann and Meixner, 2001):

$$\bar{f}^y(x,z) = \frac{1}{x\Gamma([1+m]/r)}\left(\frac{\alpha_u z^r}{r^2\alpha_K x}\right)^{[1+m]/r} \times \exp\left\{-\frac{\alpha_u z^r}{r^2\alpha_K x}\right\} \quad (16)$$

where Γ is the gamma function, and all other symbols are as defined above.

Kormann and Meixner (2001) introduced surface layer theory only at this stage, by fitting the power laws for K and $\bar{u}$ to M–O similarity relations. This Eq. (16) is an explicit algebraic relation in x and z, and thus, it constitutes the only truly analytical flux footprint model based on realistic profiles of K and $\bar{u}$ to date. Another explicit algebraic footprint expression by Hsieh et al. (2000) is a hybrid approach that fits an analytic solution to results from a numerical LS model, and is further discussed in the next section. As it does not depend on Schmidt's conjugate powers assumption, Kormann and Meixner's (2001) solution is thus both more consistent and more general than the one by Haenel and Grünhage (1999). It contains the simple solution of Gash (1986) and Schuepp et al. (1990), if an eddy diffusivity power $n = 1$ is prescribed, and is equivalent to Haenel and Grünhage (1999) if conjugate powers are assumed.

Clearly, however, the approaches of Haenel and Grünhage (1999) and Kormann and Meixner (2001) are very similar: they aimed at avoiding the inconsistent asymptotic behavior of the HW-model, and at decreasing the computational expense in practical footprint evaluations. They achieved this goal in a pragmatic way, by sacrificing physical content to mathematical simplicity. However, in today's terms, the computational expense of expressions like the HW-model is trivial, unless they need to be evaluated a large number of times. In addition, if the HW-model model is scaled by its "untheoretical" asymptotic value, to force it to unity (as is often done, in practice), the problem with the asymptotic limit is removed.

All analytical footprint models presented here assume Gaussian distributions in the crosswind direction and are restricted to surface layer scaling conditions. They also all rely on the inverted plume assumption (2). Thus, all analytical models are applicable only in areas where the profiles of K and $\bar{u}$ are horizontally homogeneous, and at heights where the effects of a finite mixing depth are negligible. In addition, all these models assume that turbulent diffusion in streamwise direction is small compared to advection, a form of Taylor's hypothesis, and are thus confined to flow situations with relatively small turbulence intensities ($I < 0.5$, suggested by Willis and Deardorff, 1976).

2.6. Forward LS flux footprint models

2.6.1. Theory

An alternative to solutions of the Eulerian advection-diffusion equation is the LS description of the trajectories of passive particles in a turbulent flow.

Its application to footprint modeling assumes that the dispersion of a passive tracer can be represented by the trajectories of a finite number of particles that are completely independent of each other. For a review of LS dispersion modeling, see e.g. Rodean (1996) or Wilson and Sawford (1996). The trajectory or time evolution of the position, x_i ($i = 1, 2, 3$) of such a particle is given by

$$\mathrm{d}x_i = u_i \,\mathrm{d}t \tag{17}$$

where u_i is the Lagrangian velocity in the x_i-direction and $\mathrm{d}t$ is a time increment. In turbulent flow, it is assumed that the Lagrangian velocity follows a first-order Markov process, as given by the Langevin equation

$$\mathrm{d}u_i = a_i(x_i, t, u_i)\,\mathrm{d}t + b_i(x_i, t, u_i)\,\mathrm{d}\xi \tag{18}$$

Here, the coefficients a_i and b_i are non-linear functions of the position, time, and velocity, and $\mathrm{d}\xi$ is a Gaussian random process with zero mean and a variance of $\mathrm{d}t$. The first term on the right represents the deterministic part of the velocity increment, and the second term is the stochastic forcing. The nature and relative weighting of these parts is given by a and b. These functions are designed to account for the stochastic nature of the turbulence field and are derived from the budget equations for the Eulerian probability density function of u_i, the Fokker–Planck equation (Thomson, 1987). In the specification of a and b, it is essential to include a drift correction term, to satisfy the well-mixed condition (Thomson, 1987). Hsieh et al. (1997) compared several different approaches to the drift correction. They conclude that cumulative footprint estimates are not very sensitive to the form of drift correction, except for unstable conditions, even though some of the approaches do not satisfy the well-mixed condition.

To consider the effect of a single particle source in isolation for footprint applications, (17) and (18) are commonly implemented with perfect reflection boundary conditions (Wilson and Flesch, 1993) at the surface and at the mixed layer height (if appropriate).

In contrast to the Eulerian models discussed above, the LS approach requires numerical integration. To obtain numerical solutions for (18), the distributions of the Eulerian flow velocities, and turbulence statistics need to be specified for the domain of the model. Thus, the structure of the turbulent flow is external to the model itself, which allows the adaptation of this approach to inhomogeneous turbulence. One of the problems discussed in the context of the analytical solutions to the Eulerian advection-diffusion equation, is the disparity between the need for realistic profiles of velocity and diffusivity, and the need for mathematical simplicity. All strategies to cope with this problem ultimately refer to (one-dimensional) similarity relationships to describe the flow and eddy diffusion profiles, and thus are constrained to homogeneous turbulence. In addition, all of them neglect turbulent diffusion in streamwise direction and are thus confined to situations where advection dominates streamwise diffusion. The primary advantage of the LS approach is that these constraints can be relaxed. In principle, LS models can account for three-dimensional turbulent diffusion and non-Gaussian inhomogeneous turbulence (e.g., Rotach et al., 1996; Reynolds, 1998). On the other hand, LS models are only as good as the turbulence representation they use to simulate the particle trajectories, and the quality of these in complex flows is often questionable.

Footprint models using the forward LS approach simulate the release of a large number of particles from a point source into a stationary turbulence field. The forward-in-time integration at discrete intervals of (18) and (17) for each of these particles provides a modeled distribution of positions and velocities. To relate this distribution to the vertical flux of material, it is assumed that the ensemble flux field in the flow is correctly represented by the modeled joint distributions of vertical velocity and position of the particles (i.e., the concentration).

The following demonstrates how footprint function values can be determined from a discrete number of LS model derived particle velocities and positions. Following van Dop et al. (1985), the ensemble concentration can be expressed in terms of a conditional probability density function for the particle cloud, so that the footprint of a measurement at $(0, 0, z_\mathrm{m})$ is (following the notation of Wilson and Swaters, 1991)

$$f(x, y, z_\mathrm{m}) = \int_0^t \int_{-\infty}^{\infty} w p(0, 0, z_\mathrm{m}, w, t | x, y, z_\mathrm{s}, t')\,\mathrm{d}w\,\mathrm{d}t' \tag{19}$$

where z_s is the source height, and $p(0, 0, z_\mathrm{m}, w, t | x, y, z_\mathrm{s}, t')\,\mathrm{d}x\,\mathrm{d}y\,\mathrm{d}z\,\mathrm{d}w$ is the probability that a particle released at (x, y, z_s, t') will at time t lie in an

elemental volume, $\mathrm{d}x\,\mathrm{d}y\,\mathrm{d}z$, centered on $(0, 0, z_m)$, with a vertical velocity of $w \pm \mathrm{d}w/2$. With a coordinate transformation equivalent to the inverse plume assumption, $p(0, 0, z_m, w, t|x, y, z_s, t')$ is equivalent to $p(x, y, z_m, w, t|0, 0, z_s, t')$. For particles released every time step $\mathrm{d}t$, from a steady state source at $(0, 0, z_s)$, $\langle w\rangle$ is the mean vertical velocity of particles that are within a finite elemental volume $(\delta x\,\delta y\,\delta z)$ centered on (x, y, z_m), and $p(x, y, z_m|0, z_s)\,\delta x\,\delta y\,\delta z$ is the probability that particles, released from $(0, 0, z_s)$ pass through the elemental volume during a time interval $\mathrm{d}t$. The discrete estimate of the footprint then becomes

$$f(x, y, z_m) = \langle w\rangle\, p(x, y, z_m|0, 0z_s)\,\delta t \tag{20}$$

Using the particle positions and velocities computed from (17) and (18), $\langle w\rangle$ and $p(x, y, z_m|0, 0, z_s)$ are obtained from

$$\langle w\rangle = \frac{1}{n}\sum_{j=1}^{n} w_j = \frac{1}{n}\sum_{j=1}^{n}\left[\left|\frac{\mathrm{d}z}{\mathrm{d}t}\right|_j \mathrm{sign}(j)\right] \tag{21}$$

$$p(x, y, z_m|0, 0z_s) \approx \frac{1}{N}\frac{\delta n}{\delta x\,\delta y\,\delta z} \tag{22}$$

where δn is the number of particles inside the elemental volume, and N is the total number of particles released at $(0, 0, z_s)$. For small time steps, $\delta t \to \mathrm{d}t$, and for an infinitesimal layer thickness, $\delta z \to \mathrm{d}z$, so that over an infinitesimal horizontal area element $(\mathrm{d}x\,\mathrm{d}y)$ centered on (x, y, z_m), the footprint value is estimated as (Hsieh et al., 2000)

$$f(x, y, z_m) \approx \frac{1}{N}\frac{\mathrm{d}^2}{\mathrm{d}x\,\mathrm{d}y} \times [n_\uparrow(x, y, z_m) - n_\downarrow(x, y, z_m)] \tag{23}$$

where $n_\uparrow$ and $n_\downarrow$ are the numbers of particles crossing level z_m within $(\mathrm{d}x\,\mathrm{d}y)$ in upward and downward direction, respectively, and $n_\uparrow + n_\downarrow = \mathrm{d}n$.

As required by the conservation of mass in (1), the integration of (23) over the horizontal plane becomes unity. In practice, the evaluation of $n_\uparrow$ and $n_\downarrow$ is performed over discrete cells of a grid, leading to a discrete footprint distribution that needs to be smoothed. As with the analytical models, footprint distributions calculated from a single point source, require the inverse plume assumption and are thus dependent on horizontal homogeneity of the turbulence field.

2.6.2. LS footprint models for flow above short vegetation

A footprint model that follows an analogous approach to (18) and (23) was first presented by Leclerc and Thurtell (1990). Their two-dimensional model considered Lagrangian dispersion in vertical direction by Gaussian turbulence, and advection with the mean flow in streamwise direction. The flow and turbulence profiles were described by standard M–O similarity relations. They presented model results of the cross-wind integrated footprint over a range of conditions and demonstrate a strong dependence on measurements height, roughness and stability (in decreasing order of magnitude). The results for neutral stability were compared to the simple analytical model by Schuepp et al. (1990), who found good qualitative agreement between the two approaches, and quantitative agreement if the Schuepp et al. (1990) model uses the local wind velocity at measurement height, rather than the layer average velocity (see (7)). Leclerc and Thurtell (1990) also presented various curves of the cumulative footprint as a function of fetch, in analogy to Gash (1986).

Horst and Weil (1992) used a similar approach, following Thomson's (1987) general stochastic model to examine their assumption of the relative insensitivity of the normalized (analytical) footprint (13) to changes in roughness and stability, if plotted against $\bar{z}/z_m$. They found excellent agreement for near-neutral conditions on both the stable and the unstable side.

The high level of agreement between the analytical and these early stochastic footprint models is not surprising, as they all essentially are adapted to M–O similarity scaling conditions in the surface layer. Indeed, Finn et al. (1996) showed in a tracer experiment that the analytical models of Horst and Weil (1992, 1994) and the stochastic models of Leclerc and Thurtell (1990) also agree, at least qualitatively, with flux measurements of a passive tracer released in a horizontally homogeneous surface layer over short vegetation. Thus, these pioneering works on stochastic footprint modeling paved the way to the high level of acceptance that the footprint approach now has in the turbulent flux measurement community. By demonstrating that the LS approach and a flux computation method like (23) is valid, they pointed towards its application to conditions that cannot be simulated by analytical models using M–O similarity profiles.

Weil and Horst (1992) presented flux footprint estimates for measurements in the convective boundary layer. They used a two-dimensional stochastic model similar to the one used in Horst and Weil (1992), but here allowed negatively skewed vertical turbulence, simulated by the superposition of two Gaussian distributions, following Sawford and Guest (1987) and Weil (1990). As their emphasis is on the convective mixed layer, they used a uniform wind velocity (U) and the mixed layer similarity profiles of turbulence statistics of Weil (1990), derived from a combination of large-eddy simulations (LESs), convection tank experiments and observations. These profiles are expressed in terms of z/z_i, the relative height in the mixed layer (z_i), and the convective scaling velocity, w_*. Particles are assumed to be perfectly reflected at the capping inversion, z_i, as well as at the surface. Although horizontal velocity fluctuations are significant in the convective mixed layer, these were ignored by Weil and Horst (1992).

Their results show self-similar footprints with a streamwise dimension (defined as the distance between the points where the footprint value falls to half of its maximum) of the order $\sim (Uz_i/w_*)(z_m/z_i)^{2/3}$. They also show that the surface layer model of Horst and Weil (1992) is able to account for convective conditions fairly well as long as the measurement height is well below $0.1z_i$. For greater measurement heights, the surface layer model grossly overestimates the growth of the mean plume height, and thus the footprint value. This is due at least in part to the effect of particle reflection at height z_i that the surface layer models ignore. It must be expected that the neglect of horizontal turbulence significantly affects the validity of Weil and Horst's (1992) results. As shown by Baldocchi (1997), the effect of horizontal turbulent diffusion is to counter the action of advection, by reducing the streamwise scale of the footprint and moving its maximum closer to the sensor. In situations where horizontal turbulence intensity is high, part of the footprint can even extend in downstream direction of the sensor (see also below).

Wilson and Swaters (1991) followed a Lagrangian framework for the surface and mixed layers, to explore the "origin" of fluid elements spotted by a sensor aloft, but then provided analytical solutions to describe the budget of various conditional particle PDFs that are interpreted as concentrations, as e.g. in (19). They differentiated between the flux and concentration footprints, defined in the usual way of (1), and introduced a "distribution of contact distance". They defined the "contact distance" as the horizontal distance, at which a fluid element that contributes to a measurement aloft, has last been in contact with the surface. To model this distribution, Wilson and Swaters (1991) assumed Gaussian turbulence, so that the surface distribution of particles released aloft is exactly reciprocal to the distribution aloft of particles released at the surface (Smith, 1957). To ensure that only the last surface contact is taken into account, they used a perfect surface absorption boundary condition (and perfect reflection at z_i). The resulting distribution of contact distance is not generally identical with the concentration footprint: the latter is also akin to a distribution of surface touchdowns, but allows for multiple touchdowns with perfect reflection. In purely Gaussian turbulence, the distribution of contact distance coincides with a concentration footprint for particles of a tracer that are perfectly absorbed upon contact with the surface. However, with this restriction, it is difficult to envision a process that would allow the surface release of the tracer in the first place. In their conclusions, Wilson and Swaters (1991) stressed the importance of properly accounting for inhomogeneous and non-Gaussian turbulence in LS modeling. According to Reynolds (1998), this goal has been achieved by Rotach et al. (1996).

Hsieh et al. (2000) presented a hybrid approach, combining elements from Calder's (1952) analytical solution with results from an LS model. They used Thomson's (1987) model, with turbulence considered in the vertical only, to estimate the flux footprint according to a crosswind integrated version of (23) over a range of stabilities, roughness lengths and measurement heights. In the analysis of their results, they non-dimensionalized Gash's (1986) effective fetch (6) by the Obukhov length, and accounted for the effects of stability by the introduction of two similarity parameters, D and P, so that

$$\frac{x_F}{|L|} = -\frac{1}{k^2 \ln(F)} D \left(\frac{z_u}{|L|} \right)^P \tag{24}$$

where $z_u = z_m(\ln(z_m + z_0) - 1 + z_0 + z_m)$ follows from the layer-averaged logarithmic wind profile as an expression for U in (6). The parameters D and P are found by regression of (24) to the stochastic model results for unstable ($D = 0.28$; $P = 0.59$), near-neutral

($D = 0.97$; $P = 1$), and stable ($D = 2.44$; $P = 1.33$) stratification. Rearrangement and differentiation of (24) with respect to x leads to an approximate analytical expression for the footprint (compare (7))

$$f(x) = \frac{1}{k^2 x^2} D x_u^P |L|^{1-P} \exp\left[-\frac{1}{k^2 x} D z_u^P |L|^{1-P}\right] \quad (25)$$

A comparison of (25) with the numerical stochastic results and with the analytic model of Horst and Weil (1992) show good agreement in near-neutral conditions, and agreement of the peak footprint location within an order of magnitude of x for unstable and stable conditions. In Hsieh et al. (2000), the similarity parameters D and P are optimized for the integral flux expression (24). The agreement with the stochastic model of both the peak location and the streamwise extent of the footprint could possibly be enhanced, if the parameters were optimized for the differential footprint expression (25) instead.

2.6.3. LS footprint models for flow over tall vegetation

The first footprint model to be developed for use within and over vegetation canopies was presented by Baldocchi (1997). The LS model he used is based on (18) and Thomson (1987), with Gaussian turbulence described by Eulerian statistics for neutral conditions. Compared to flow over uniform, short vegetation, only very few generally valid characteristics of turbulence in and directly over a tall canopy are known (Kaimal and Finnigan, 1994; Finnigan, 2000). Specifically, no equivalent similarity theory to organize empirical knowledge from a variety of sites is available for canopy flow. This lack of a unified theoretical framework leads to the need for crude generalizations and sometimes inconsistent ad hoc assumptions in the description of canopy turbulence. Some of the resulting difficulties are discussed below.

To account for the flow and turbulence characteristics through a forest canopy, Baldocchi (1997) implemented two discrete horizontally homogeneous layers that are matched at the canopy height, h. The upper part is a standard surface layer with a logarithmic wind profile, with a zero plane displacement length of $d \propto h$. The ratios of $\sigma_{w,u}/u_*$, where $\sigma_{w,u}$ are the standard deviations of vertical and streamwise velocity fluctuations, are height invariant (neutral conditions). The canopy layer is implicitly assumed to have a uniform vegetation density distribution. Thus, the mean wind velocity $\bar{u}(z)$ and $u_*(z)$ in the canopy are assumed to reduce exponentially from their values at canopy height, following Cionco (1978) and Uchijima and Wright (1964). Following Raupach (1988), $\sigma_{w,u}/u_*(z)$ are approximated to decrease linearly with depth. The Lagrangian time scale, T_L, in the surface layer is assumed to increase linearly with height, $T_L = k(z-d)/(1.25u_*)$, while it is treated as invariant with height in the canopy, $T_L = 0.3h/u_*(h)$, following Raupach (1989). It should be noted that, with these formulations, T_L has a discontinuity at the canopy height.

Baldocchi (1997) showed that the effects of streamwise turbulence cannot be neglected in canopy flow, where turbulence intensity increases with depth below h. Streamwise turbulence reduces the extent of the footprint and moves its peak downwind considerably. Similarly, the canopy flux footprint for sources on the forest floor is shown to be much contracted compared to those evaluated in the surface boundary layer. Baldocchi (1997) only considered the footprint for sources on the forest floor, but his model can easily be adapted to source locations at any height within the canopy layer.

Rannik et al. (2000) built on the approach of Baldocchi (1997) and presented a footprint model for forest canopies based on a three-dimensional LS model. This model follows (18), and satisfies the well-mixed condition, but follows Kurbanmuradov and Sabelfeld (2001) for the determination of a and b. They used Gaussian turbulence in neutral or unstable conditions and separated the flow into three sub-layers: a surface layer, where M–O scaling applies, a roughness sublayer below a height z_*, and a canopy layer below the canopy height h. The parameterization of the flow statistics follows standard M–O similarity relations for the surface layer. The mean velocity and its vertical gradient in the roughness sublayer are treated following Cellier and Brunet (1992), and inside the canopy layer, an exponential decrease is assumed, as in Baldocchi (1997). For the velocity standard deviations ($\sigma_{u,v,w}/u_*$) no roughness sublayer is considered, and the stability dependent standard surface layer relation links directly to a linear decrease form the value at h in the canopy layer, as in Baldocchi (1997). Similarly, the vertical momentum flux is constant above h and decreases exponentially in the canopy (see Baldocchi,

1997). The only second-order statistic where a three layer approach is followed, is the dissipation rate, ε. Here an asymptotic matching function is used to link the surface layer profile (above z_*) to an assumed value at h. Below h, ε is reduced, using an ad hoc function to simulate the qualitative behavior of ε in canopy flow reported in Kaimal and Finnigan (1994).

The vertical gradients of the mean velocity are available in analytical form in Rannik et al. (2000) for the three sublayers. However, as in Baldocchi (1997), the gradient profiles are discontinuous at the canopy height. A forthcoming sensitivity analysis by M.G. Villani (personal communication) demonstrates that such profile discontinuities at the canopy height affect the resulting footprint peak values by 30% or more for scenarios where the principal exchange is with sources (or sinks) at the canopy height.

Both Baldocchi (1997) and Rannik et al. (2000) used state-of-the-art turbulence parameterizations through the canopy. Thus, the inconsistencies of these parameterizations are more indicative of the lack of a unified framework to describe turbulence statistics in and above vegetation canopies, than deficiencies of these models. Nevertheless, Rannik et al. (2000) presented interesting results that are significant for future developments of footprint modeling over forest canopies.

They compared the footprints for various source configurations, namely sources at the forest floor, at canopy height, and a distributed source proportional to the vertical profile of leaf area density. As expected, the peak of the canopy-top footprint is much steeper and closer to the sensor than the forest floor footprint, because the vertical separation between source and sensor is smaller for the canopy source. However, the peak distance of the distributed source footprint is not significantly different from the canopy-top release, but it is much broader and its upwind tail approaches that of the forest floor release. For a relatively low measurement height of $z/h = 1.7$, a considerable portion of all three of these footprint estimates comes to lie downwind of the sensor, due to the effect of streamwise turbulence. They also evaluated the sensitivity of the importance of in-canopy flow to measurement height, compared to a pure atmospheric surface layer (ASL) footprint with an effective release height at $z_m = d + z_0$. In essence, this sensitivity test explores the importance of accounting for the characteristics of the flow and turbulence inside and below the forest canopy, with a model such as Baldocchi (1997) or Rannik et al. (2000), as opposed to the use of (e.g.) one of the analytical footprint models discussed above. These comparisons are presented for three measurement heights: $z_m/h = 1.3, 2, 4$. For measurements close to the canopy-top, the "forest" characteristic is quite pronounced, and especially the upwind tail of the footprint is underestimated by the ASL models. For measurements higher above the forest, the two model approaches converge, but Rannik et al. (2000) showed that streamwise turbulence remains important even for measurement heights exceeding $z_m/h = 4$. A portion of the footprint extends downwind of the sensor, even for the ASL model, but the relative amount decreases with measurement height.

All models and approaches for flux footprint calculations discussed so far rely on the inverse plume assumption (2) and thus are valid only in horizontally homogeneous flow. Luhar and Rao (1994) explored the variations in footprint estimates, if the footprint is allowed to develop in an internal boundary layer following a step change in surface roughness and surface moisture. Turbulence and flow statistics were provided by a second-order closure model. Obviously, the inverse plume assumption (2) cannot be used in this situation. In their two-dimensional framework, Luhar and Rao (1994) handled this problem by simulating up to 30 surface line sources, located at various distances downwind of the step change. Each of these line sources was set to release 10^4 particles and modeled with the two-dimensional LS model by Luhar and Britter (1989). Luhar and Rao (1994) reported good agreement between the fluxes evaluated from the footprint estimates, using (1), and those evaluated by the second-order closure model. This result raises confidence in the robustness of the footprint concept, even for extensions to horizontally inhomogeneous conditions. However, it comes at the expense of a significant increase in computational expense, in direct proportion to the number of sources needed to describe the developing flux field.

2.7. Backward LS flux footprint models

Flesch et al. (1995) introduced a backward-in-time LS dispersion approach for fluid particles, in analogy to the well-known back-trajectory approach of

non-mixing air columns at the synoptic scale. They showed that the backward-time Langevin equation, equivalent to the pairs (17) and (18), is achieved by a simple linear coordinate transformation, so that $t \rightarrow t'$, where $t' = T_0 - t$, and T_0 is an arbitrary constant. The backward-time conditional probability densities that lead to the corresponding functions a' and b' in the backward equivalent of (18) are shown to be given by a Fokker–Planck equation that differs from the forward version only by a sign change in the second-order term (for details, see Flesch et al., 1995).

The turbulent dispersion of a scalar in a continuum consists of an infinite number of trajectories. The forward LS approach randomly samples a subset of trajectories emanating from a single point source, or from a finite number of point sources at pre-defined locations. The backward-time LS approach considers only those trajectories that pass through a pre-defined sensor location, but is not limited to any particular number or distribution of potential sources for the material carried along those trajectories. Both approaches assume that the finite number of trajectories, simulated by the model, describe the ensemble behavior of the dispersing scalar material. A subtle difference exists in interpretation of the dispersing "particles": in the forward approach, such a "particle" is often considered as a place-holder for a given amount of the dispersing scalar material. The incremental "mass loading" of a forward particle, $\delta m_j^{\mathrm{f}}(\mathbf{x}_0)$, released from an incremental area δa at location $\mathbf{x}_0$, is simply proportional to the surface source strength, Q_0, so that

$$\delta m_j^{\mathrm{f}}(\mathbf{x}_0) = \frac{Q_0}{N}\delta a\,\delta t \tag{26}$$

where N is the number of particles released over a time step δt. Thus, in the forward mode, each particle carries the same amount of mass. In contrast, the dispersing "particles" in the backward approach are viewed simply as fluid elements, or parcels, that are not necessarily charged with any scalar mass, but may have varying amounts. Fluid elements passing through the sensor location $\mathbf{x}_0$ at time $t = 0$ receive this scalar charge only if they reside within a source volume δV over a residence time t_j at location $\mathbf{x}$, with volumetric source strength $S_0(\mathbf{x})$, at any time $t < 0$

$$\delta m_j^{b}(\mathbf{x}, t|\mathbf{x}_0, 0) = S_0(\mathbf{x})\tau_j\,\delta V \tag{27}$$

Trajectories that reach the sensor without ever impacting on a source, are thus not charged with any scalar mass. For a surface source $Q_0 = S_0\,\mathrm{d}z$, the residence time can be expressed in terms of a "touchdown velocity" w_j^{T}, so that $\tau_j = 2\,\mathrm{d}z/|w_j^{\mathrm{T}}|$, where the factor two implies reflection at the surface. In this case, the incremental mass charge of a fluid element, upon touchdown at a source, is inversely proportional to its touchdown velocity. A given fluid element may score several touchdowns, each time receiving an additional incremental scalar charge, before reaching the sensor location. Thus, the ensemble concentration at the sensor location, due to an elemental source centered on $\mathbf{x}$ becomes (Flesch et al., 1995)

$$\bar{C}(\mathbf{x}_0) = \frac{1}{N}\sum_{j=1}^{N}\sum_{i=1}^{N_{Td}^{j}}\frac{\delta m_{j,i}^{b}(\mathbf{x}|\mathbf{x}_0)}{\delta V} = \frac{Q_0(\mathbf{x})}{N}\sum_{j=1}^{N}\sum_{i=1}^{N_{Td}^{j}}\frac{2}{|w_{j,i}^{\mathrm{T}}|} \tag{28}$$

where $w_{j,i}^{\mathrm{T}}$ is the velocity of "i"th touchdown within the elemental source, by the "j"th fluid element.

Flesch (1996) proposed to use the backward-time LS approach to compute the flux footprint for a given sensor location, based on a large number of back-trajectories. Following Flesch et al. (1995), and (28) the vertical flux at the sensor location ($\mathbf{x}_0$) due to all sources within an elemental surface area, δa, becomes

$$F(\mathbf{x}_0) = \overline{C(\mathbf{x}_0)w(\mathbf{x}_0)} = 2\frac{Q_0(\mathbf{x})}{N}\sum_{j=1}^{N}\sum_{i=1}^{N_{Td}^{j}}\frac{w_j(\mathbf{x}_0)}{|w_{j,i}^{\mathrm{T}}|} \tag{29}$$

The velocity $w_j(\mathbf{x}_0)$ refers to the sensor location and is thus the initialization velocity of the "j"th fluid element, w_j^{ini}. With (29) and (1) the flux footprint is estimated by a backward-time LS model as

$$f(\mathbf{x}) = \frac{2}{N\,\delta a}\sum_{j=1}^{N}\sum_{i=1}^{N_{Td}^{j}}\frac{w_j(\mathbf{x}_0)}{|w_{j,i}^{\mathrm{T}}|} \tag{30}$$

In (30), the $\mathbf{x}$-dependence of the footprint is implied in the location at which the touchdowns occur.

In homogeneous flow, the forward and backward approaches are equivalent (Flesch et al., 1995). However, the most significant advantage of the backward approach is that it obtains the footprint distribution directly, without depending on an inverse plume

assumption (2). The backward approach is thus a potentially very efficient method to estimate a flux footprint in horizontally inhomogeneous flow (Kljun et al., 2000b). An additional benefit of the backward approach is that, for a given sensor location, any source geometry may be considered in post-processing, without the need to re-run the model, if the trajectory positions and velocities are stored. The "residence time" concept can easily be expanded to reference surfaces (or infinitesimal layers) away from the surface (e.g. at varying levels in a vegetation canopy) where the fluid element is not reflected, but moves according to the given velocity statistics. In contrast, the model needs to be re-run for every new sensor height, whereas in the forward approach, the footprint adjustment to different sensor heights can be achieved in post-processing, albeit only in horizontally homogeneous conditions.

The backward LS approach to flux footprint modeling is relatively new, and only little experience with it has accumulated since the publication of Flesch (1996). Kljun et al. (1999, 2000a,b, 2002) have adopted the three-dimensional version of the LS model by Rotach et al. (1996) to run in backward-time mode. This model is unique in that it is able to simulate a continuous range of stabilities from stable to convective, while satisfying the well-mixed condition of Thomson (1987) everywhere. Kljun et al. (1999, 2000a,b, 2002) demonstrated the qualitative and quantitative equivalence of their backward LS footprint estimates to simple analytical schemes, such as Horst and Weil (1992) and the flux source area of Schmid (1994, 1997), if the model conditions are similar. Kljun et al. (2002) addressed some of the challenges of backward LS footprint modeling in detail.

As seen in (30), the footprint depends critically on the initialization of the vertical velocity distribution at the sensor location (i.e., the backward "release point"). It turns out that the correct correlation between vertical and streamwise velocity fluctuations is crucial in this context. The construction of initial velocity distributions that comply to measured single and joint probability distributions is not trivial for all atmospheric stabilities. This is achieved by letting the model tune itself, by building up the distributions in a "spin-up" period, before the trajectories are launched. In this spin-up, velocity increments are computed according to the backward version of (18), but the corresponding incremental displacements (17) are ignored, so that the particles are essentially idling on the sensor point.

Kljun et al. (2002) demonstrated that the backward LS footprint approach of Flesch (1996) has matured sufficiently for the development of applications in horizontally inhomogeneous or non-stationary flow and turbulence configurations. If such developments are successful, they hold the promise of significant progress towards an efficient footprint model that is applicable in realistic flow and vegetation canopy geometries.

2.8. LES-based approach to footprint modeling

In principle, any two- or three-dimensional model that solves the Navier–Stokes equations and some form of conservation of mass equation, with suitable initial and boundary conditions, can be used to compute the dispersion of a scalar from arbitrary sources, and the footprint of a reference location in the model domain. In particular, LES models (e.g., Mason, 1994) can provide a nearly complete representation of the essential flow structures responsible for scalar transport, depending on the model resolution and the order of closure at the subgridscale. The operation of LES models is extremely resource intensive, with respect to computer CPU time, memory and storage capacity, and post-processing effort. This computational expense typically grows with the third to fourth power of the model resolution (spatial and temporal), and therefore with the degree to which horizontal or vertical inhomogeneities are resolved. Thus, in practice, most LES applications in the atmospheric boundary layer have been limited to idealized surface configurations, with periodic boundary conditions, and simple or highly symmetric inhomogeneities. They typically perform best in convective conditions, when large-eddy structures are dominant. These are also the conditions where ensemble average models (particularly *K*-theory models) perform notoriously badly.

In this sense, LES models (and also higher-order ensemble average models) are in a different class of models from the footprint models we have discussed so far. For a given model scenario, such models can simulate both the turbulence statistics, and the scalar flux field that results from them. In contrast, conventional footprint models, evaluate the scalar flux field based on imposed turbulence statistics (LS-based

models) or based on a ensemble closure assumption (*K*-theory) and imposed mean similarity profiles (analytical models). The high computational expense of LES applications makes their use for routine diagnostic footprint evaluations impractical. However, as research and development tools, LES-based footprint computations can be extremely valuable. They can serve to cross-compare and validate other footprint models, or to provide the flow and turbulence statistics to drive LS-based footprint models. Particularly in conditions where the flow and turbulence field is not well-described by self-similar profiles (e.g., forests, inhomogeneous areas, roughness sublayers, convective conditions), LES-based turbulence statistics can be invaluable.

The first LES application to footprint modeling is by Hadfield (1994). In this work, a horizontally homogeneous LES for convective conditions produces the velocity field to drive a forward LS footprint model. Lagrangian particle velocities are composed of a resolved part and a subgrid part. The resolved part is interpolated from the gridded LES velocity field, and the subgrid part uses the subgrid kinetic energy to construct an LS model that satisfies the well-mixed condition, following Legg and Raupach (1982). The vertical flux distribution in the lower portion of the boundary layer ($z_m/z_i = 0.18$) due to a continuous surface point source agrees qualitatively with analytical footprint models, such as the HW-model or Schmid (1994). Hadfield (1994) also considered the flux distribution due to various scalar source distributions. However, as the turbulence field remains unchanged, the footprint itself is not affected by that.

Leclerc et al. (1997) used a slightly different approach. They used the LES model of Moeng (1984) and added a passive scalar equation. They initially spun-up the model without any scalar dispersion, until it had reached a quasi-steady state, with a mean velocity of U along the x-axis. Instead of a point source and the computation of Lagrangian trajectories, like in Hadfield (1994), they followed Nieuwstadt and de Valk (1987) and released an instantaneous surface line puff along the streamwise axis, with a cross-section of one grid cell. With $x = U/t$, the time evolution of the scalar dispersion due to the instant line puff is equivalent to the streamwise development of a continuous elemental volume source. However, with only a mean streamwise velocity used for the coordinate transformation, the effects of streamwise turbulence are neglected. Thus, in Leclerc et al. (1997) the dispersion of the scalar is entirely simulated in a Eulerian framework by the LES model, without the need for an embedded LS model. The crosswind integrated flux footprint then follows directly from $\overline{f^y}(x) = \mathrm{d}\overline{F^y}/\mathrm{d}x$. Leclerc et al. (1997) compared this LES footprint with the analytical model of Horst and Weil (1992), the LS model of Leclerc and Thurtell (1990), and results from the tracer release of Finn et al. (1996). The agreement between the models is very good in the upper part of the surface boundary layer (∼10% z_i). Closer to the surface, the subgrid effects of the LES become significant, but at $z_m = 10$ m, where the tracer flux measurements are available, the agreement is still within the uncertainty of the measurements. There is some indication that the peak of the measured fluxes lies closer to the source than predicted by either of the models. As none of the models compared here account for streamwise turbulence, it is expected that their footprints are too far upstream (see, e.g., Rannik et al., 2000; Kljun et al., 2002).

Su and Leclerc (1998) used the LES of Su et al. (1998) for neutral stability flow in a forest canopy and the surface layer above, to evaluate scalar dispersion from sources at three different heights in the canopy layer and at the forest floor. The model domain is homogeneous in both horizontal directions and the sources are simulated as infinite spanwise lines with a cross-section of one grid cell. Instead of releasing an instantaneous puff, as in Leclerc et al. (1997), these sources are treated as continuous. For measurement heights below the source the footprint is negative at small distances, as expected, and then becomes slightly positive at greater distances. Qualitatively, the footprints due to sources below the measurement height correspond closely to those presented by Baldocchi (1997) and Rannik et al. (2000). For the forest floor source Su and Leclerc (1998) reported a double maximum of the flux footprint. However, this is not likely a significant result, but rather reflects the stochastic nature of all LESs, if the spanwise and temporal integration is finite (H.-B. Su, personal communication).

Both Leclerc et al. (1997) and Su and Leclerc (1998) concluded that these early applications of LES to footprint modeling confirm the general validity of the approach. Further simulations are needed to evaluate the influence of variable canopy morphology,

horizontal heterogeneity of the flow, and inhomogeneous buoyancy. Such future studies will stretch the currently available computer resources considerably, but signify progress into an area where LES models are possibly the only solution.

The main characteristics of all footprint modeling approaches discussed here are summarized in Table 1. The order of presentation in Table 1 is chronological. The more recent model approaches tend to have more skills to simulate footprints in realistic experimental conditions, and are thus more resource intensive. However, the interest in simple analytical models permeates this development throughout.

3. Biosphere–atmosphere exchange and the footprint concept

The previous sections have dealt with technical aspects of modeling the footprint of a turbulent flux measurement. The question remains, if and how footprint models can be useful in experimental studies of biosphere–atmosphere exchange.

Although ecosystem–atmosphere exchange happens at the material interface between plant tissue (or soil) and ambient air, it is often most convenient to infer the net ecosystem exchange from turbulent flux measurements at height, above the vegetation canopy. Techniques to measure the interfacial exchange directly exist (various enclosure techniques), but difficulties associated with maintaining ambient conditions in an enclosure, or scaling up to the ecosystem often prove insurmountable. A comparison of the so-called ecological and micrometeorological methods to estimate ecosystem exchange is presented in Ehman et al. (2002). While micrometeorological flux measurements avoid these problems of interference and (to a certain extent) scaling, other concerns arise because of the separation between the turbulent flux sensors and the active surface of the exchange. The following section discusses the utility and limitations of footprint models to determine how ecosystem exchange is expressed in measured turbulent fluxes.

3.1. Flux measurements and mass conservation over tall vegetation

The connection between the turbulent flux measurement of a trace gas, C, and its biosphere–atmosphere exchange at the interface is given by the mass conservation equation over a volume V. For convenience, this control volume is commonly taken to be a rectangular box ($\pm\delta x, \pm\delta y, \delta z = z_\mathrm{m}$), centered on an arbitrary origin, up to the height of the flux sensor, z_m. The conservation equation can then be written in tensor notation with the usual summation convention:

$$\mathrm{NEE_C} = \frac{z_\mathrm{m}}{V}\int_{-\delta x}^{+\delta x}\int_{-\delta y}^{+\delta y}\int_{0}^{z_m} \times\left[\frac{\partial \bar{C}}{\partial t} + \frac{\partial \bar{u}_i \bar{C}}{\partial x_i} + \frac{\partial \overline{u'_i C'}}{\partial x_i} + R_\mathrm{C}\right]\mathrm{d}x\,\mathrm{d}y\,\mathrm{d}z \tag{31}$$

In (31), overbars denote ensemble averages, primes are deviations from the average, $\mathrm{NEE_C}$ is the net ecosystem exchange of C at the vegetation/soil–air interface, averaged over the horizontal area of the box (z_m/V), and R_C denotes net chemical sources or sinks of C in the air volume. The terms in (31), from left to right, indicate that $\mathrm{NEE_C}$ is balanced by the storage change of C in the box, the mean mass flow divergence components, turbulent transport, and any transformations occurring in the air volume of the box. This equation can be somewhat simplified without much loss of generality. The flux at the interface is given by the left-hand side (LHS) of (31), so that the turbulent flux at the lower boundary vanishes. If mean horizontal advection is considered much larger than the horizontal divergence of the turbulent flux, the turbulent flux term reduces to the horizontal integral of $F_\mathrm{C}(z_\mathrm{m}) = \overline{w'C'}$ over ($\pm\delta x$, $\pm\delta y$). Here, we will not consider gas species that are chemically reactive in the atmosphere, so that the last term in (31) is neglected. If x is aligned with the horizontal streamwise direction (u), advection reduces to a streamwise term and a vertical term. Using the incompressible continuity, (31) becomes

$$\mathrm{NEE_C} = \frac{z_m}{V}\int_{-\delta x}^{+\delta x}\int_{-\delta y}^{+\delta y} \times\left(\int_{0}^{z_m}\left[\frac{\partial \bar{C}}{\partial t} + \bar{u}\frac{\partial \bar{C}}{\partial x} + \bar{w}\frac{\partial \bar{C}}{\partial z}\right]\mathrm{d}z + F_\mathrm{C}(z_m)\right)\mathrm{d}y\,\mathrm{d}x \tag{32}$$

Sensors for turbulent flux measurements are ideally placed above an area that is homogeneous

Table 1
Summary of footprint model characteristics

Model (principal reference)	Inverted plume	Inhomogeneous[a]		u'[b]	Domain[c] (height range)	Solution approach[d]	Assumed profiles[e]	Remarks
		Horizontal	Vertical					
Pasquill (1972)	Yes	No	No	No	ASL	Analytic	Uniform	Conc.[f]
Gash (1986)	Yes	No	No	No	N-ASL	Analytic	Uniform	
Schmid and Oke (1990)	Yes	No	No	No	US-ASL	Analytic, SA	M–O	Conc.
Schuepp et al. (1990)	Yes	No	No	No	N-ASL	Analytic	Uniform	
Leclerc and Thurtell (1990)	Yes	No	Yes	No	ASL	LS (F)	M–O	
Wilson and Swaters (1991)	Yes	No	Yes	No	ASL/C-ML	LS (F)	M–O/CML	Contact dist.
Horst and Weil (1992, 1994)	Yes	No	No	No	ASL	Analytic	M–O	
Weil and Horst (1992)	Yes	No	No	No	C-ML	LS (F)	CML	
Hadfield (1994)	Yes	No	Yes	Yes	C-ABL	LES + LS (F)	None	
Luhar and Rao (1994)	Yes	Yes	Yes	Yes	ASL	LS (F)	II closure	Multi source
Schmid (1994)	Yes	No	No	No	ASL	Analytic, SA	M–O	
Flesch (1996)	No	Yes	Yes	No	N-ABL	LS (B)	M–O	
Leclerc et al. (1997)	No	Yes	Yes	No	C-ABL	LES	None	
Stannard (1997)	Yes	No	No	No	ASL	Analytic	M–O	β
Baldocchi (1997)	Yes	No	Yes	Yes	FCL + N-ABL	LS (F)	Empir. +M–O	Forest
Su and Leclerc (1998)	No	Yes	Yes	Yes	FCL + N-ASL	LES	none	forest
Horst (1999)	Yes	No	No	No	ASL	analytic	M–O	profile, β
Haenel and Grünhage (1999)	Yes	No	No	No	ASL	analytic	power/M–O	
Hsieh et al. (2000)	Yes	No	No	No	ABL	hybrid	M–O	LS (F) + regr.
Rannik et al. (2000)	Yes	No	Yes	Yes	FCL + RSL + ASL	LS (F)	Empir. + M–O	Forest
Kormann and Meixner (2001)	Yes	No	No	No	ASL	Analytic	Power/M–O	
Kljun et al. (2002)	No	Yes	Yes	Yes	ASL + C-ML	LS (B)	M–O + CML	

[a] This reflects the *potential* of the model to include horizontal or vertical inhomogeneity in the flow and turbulence field.

[b] Streamwise turbulence/diffusion.

[c] ASL: atmospheric surface layer; ABL: atmospheric boundary layer; ML: mixed layer; FCL: forest canopy layer; RSL: roughness sublayer; N: neutral; US: unstable; C: convective.

[d] LS: Lagrangian stochastic; F: forward; B: backward; LES: large-eddy simulation; SA: source area.

[e] Assumed profile shapes for mean velocity and diffusivity or turbulence statistics.

[f] Conc.: for concentration only; β: Bowen ratio; regr.: regression.

in its surface coverage and has flat terrain. Over such a surface, any horizontal gradients disappear, the surface–atmosphere exchange is only relevant in the vertical, and the vertical direction coincides with the direction that is normal to the terrain and normal to the mean flow. This is the ideal situation where M–O similarity theory applies, and vertical fluxes are considered invariant with height over a range of approximately $z_* \geq z_m \geq 0.1 z_i$ (where z_* is the height of the roughness sublayer, see, e.g., Raupach et al. (1991), and z_i is the depth of the daytime mixed layer). Within this height range, flux measurements are insensitive to the horizontal or vertical placement of the sensor. Eq. (32) reduces to just two terms on the right-hand side (RHS): storage change and vertical turbulent flux through the lid of the box. Over tall vegetation, storage change is often non-negligible at hourly time-scales or less, but can relatively easily be assessed by the time increments of vertical profile measurements (e.g., Goulden et al., 1996; Schmid et al., 2000). In steady state and horizontally homogeneous conditions, the storage change term disappears as well and the interfacial biosphere–atmosphere exchange is given directly by the turbulent flux aloft

$$\mathrm{NEE_C} = F_C(z_m) \tag{33}$$

However, over naturally vegetated surfaces, variability and inhomogeneity are the rule. Most long-term flux measurements are done in locations with varying degrees of topography and variations in vegetation or land-use over horizontal scales of 10^3 m or less. The fact that (33) is thus clearly not valid in most practical situations underlines the need to consider (32), or even (31) as the basis for assessing biosphere–atmosphere exchange (Baldocchi et al., 2000).

Typically, flux measurements are conducted on a single tower so that the spatial integration required in (32) is not technically feasible. However, micrometeorological flux sensors respond to an aggregate of surface conditions contained in their flux footprint (Schuepp et al., 1990). The dimensions and orientation of the flux footprint depend on the location and height of the sensor, and vary in time with stability and wind direction. In essence, over the averaging time of a flux calculation, the flux is determined by the covariance of concentration and vertical velocity in the sequence of turbulent eddies that are advected past it, and the footprint describes the region of the surface that affects the concentrations and velocities of these eddies. Thus, to accept a time-averaged flux as a valid estimate of biosphere-atmosphere exchange over an area of $A = (4\,\delta x\,\delta y)$, we implicitly rely on the following ergodic hypothesis:

$$\begin{aligned}\frac{1}{A}\int_{x-\delta x}^{x+\delta x}\int_{y-\delta y}^{y+\delta y}\phi(\tilde{x},\tilde{y},z,t)\,\mathrm{d}\tilde{y}\,\mathrm{d}\tilde{x}\\ = \langle\phi(x,y,z,t)\rangle^A = \frac{1}{2\tau}\int_{t-\tau}^{t+\tau}\phi(x,y,z,\tilde{t})\,\mathrm{d}\tilde{t}\\ = \bar{\phi}(x,y,z,t)\end{aligned} \tag{34}$$

where 2τ is the averaging period of the flux measurement. The spatial and temporal averaging filter operators, $\langle\rangle^A$ and $\overline{()}$ are defined by (34). In the formulation of (32) and (34), the spatial filter is a box-car, with a uniform weight ($1/A$) over the entire domain, as is appropriate for modeling of biosphere–atmosphere exchange. However, as shown by Horst and Weil (1992) and Schmid (1994), the sensor footprint is a smooth weight-distribution function of a spatial filter that approaches zero asymptotically on all sides, $f_\phi(x,y,z,\tilde{x},\tilde{y})$, where $\tilde{x}$, $\tilde{y}$ are dummy variables for a given combination of (x,y,z), to anticipate that the filter function itself may be spatially inhomogeneous. We thus need the additional assumption that

$$\begin{aligned}\frac{1}{A}\int_{x-\delta x}^{x+\delta x}\int_{y-\delta y}^{y+\delta y}\phi(\tilde{x},\tilde{y},z,t)\,\mathrm{d}\tilde{y}\,\mathrm{d}\tilde{x}\\ = \int_{x-\infty}^{x+\infty}\int_{y-\infty}^{y+\infty} f_\phi(x,y,z,\tilde{x},\tilde{y})\phi(\tilde{x},\tilde{y},z,t)\,\mathrm{d}\tilde{y}\,\mathrm{d}\tilde{x}\end{aligned} \tag{35}$$

or, formulated as a probabilistic representativeness criterion, and using the angular brackets $\langle\rangle$ as the spatial averaging operator,

$$\begin{aligned}\mathrm{Pr}\left\{\frac{(\langle\phi(x,y,z,t)\rangle^A - \langle\phi(x,y,z,t)\rangle^{f_\phi})^2}{(\langle\phi(x,y,z,t)\rangle^A)^2} \leq \delta^2\right\}\\ = \Pi\end{aligned} \tag{36}$$

where Π is the probability (Pr) that the footprint average of f differs from the control area average by no more than a fraction d. In (36), the footprint filter function retains an index 'ϕ', to allow for a dependence of f_ϕ on the quantity 'ϕ' that is being averaged. Obviously, the validity of any measured flux

or concentration as reflecting biosphere–atmosphere exchange in the framework of (32) hinges critically on the criterion in (36). This argument leads to one of the central requirements of biosphere–atmosphere exchange measurements over inhomogeneous areas: the weighted average biosphere–atmosphere exchange contained in the sensor footprint for any measured quantity, ϕ, in (32), must be representative of the source/sink activity contained in the box, V, of (32). In this sense, (36) is a spatial representativeness argument that is equivalent to the notion of footprint representativeness developed in Schmid (1997). Methods to assess (36) quantitatively are given in Schmid (1997) and Schmid and Lloyd (1999).

Following Mahrt (1987), the footprint-weighted spatial averaging of exchange processes over inhomogeneous areas leads to additional dispersive terms, arising from correlations between deviations from the spatial average. Thus, the total vertical exchange of C in a block time-averaging scheme becomes

$$\langle\overline{wC}\rangle = \langle\bar{w}\rangle\langle\bar{C}\rangle + \langle\bar{w}''\bar{C}''\rangle + \langle\overline{w'C'}\rangle + \langle\langle\bar{w}\rangle\bar{C}''\rangle + \langle\bar{w}''\langle\bar{C}\rangle\rangle \quad (37)$$

where $()''$ denotes a local deviation from the spatial average. In (37), the LHS is the total vertical C-exchange. The first term on the RHS represents the mean advection by the spatially averaged vertical velocity. The second term is the dispersive flux due to the spatial correlation of the local time averages. The third term is the footprint-averaged turbulent flux, and the last two terms are Leonard terms (Leonard, 1974) that do not generally vanish if the mean w-field and the mean C-field are inhomogeneous (similar cross-terms with single deviations in time vanish in the block time-average here). Assuming that the Leonard terms are small compared to the dispersive flux, (34), (36), and (37) can be combined with (32) to give

$$\mathrm{NEE_C} = \int_0^{z_s} \left[\frac{\partial\langle\bar{C}\rangle}{\partial t} + \langle\bar{u}\rangle\frac{\partial\langle\bar{C}\rangle}{\partial x} + \langle\bar{w}\rangle\frac{\partial\langle\bar{C}\rangle}{\partial z} + \frac{\partial\langle\bar{w}''\bar{C}''\rangle}{\partial z} + \frac{\partial\langle\bar{u}''\bar{C}''\rangle}{\partial x} \right] \mathrm{d}z + \langle F_C(z_s)\rangle \quad (38)$$

The last term on the RHS of (38) is the measured turbulent flux averaged over a space domain defined by the flux footprint. If the weighted average of the surface elements covered by the flux footprint is representative of the ecosystem type, the turbulent flux is spatially representative and (36) is satisfied for this term. Methods to evaluate the spatial representativeness of flux footprints quantitatively are discussed in Schmid (1997) and Schmid and Lloyd (1999). The flux footprint approach does not directly address the averaging domain of the other terms on the RHS of (38), and thus their influence and relationship to the footprint averaging domain must be carefully considered. This is done in the following.

3.2. Footprint considerations in the mass conservation equation

The fourth and fifth terms on the RHS of (38) are the dispersive fluxes. These are non-canceling local perturbations of the advective terms. Within and close to the inhomogeneous canopy their overall contribution can be large, but above the rough canopy the high levels of turbulence is expected to smooth out much of the systematic spatial perturbations (Finnigan, 2000). The height up to which a perturbation in the dispersive flux can persist may be estimated by the diffusion height scale, z_D, following Claussen (1989), as

$$z_D - d = \frac{u_*}{\hat{U}(z_D)}\lambda \quad (39)$$

where d is the zero plane displacement length, u_* the friction velocity, $\hat{U}$ the layer-averaged scalar wind magnitude up to height z_D and λ is the length scale of the surface perturbations. Using a logarithmic profile to evaluate $\hat{U}$ for $z_D \gg z_0 + d$, the roughness length, (39) is approximated by

$$z_D - d \approx \frac{\lambda}{k}\left[\ln\left(\frac{z_D - d}{z_0}\right) - 1 - \Psi_m\right] \quad (40)$$

where k is von Kàrmàn's constant, and Ψ_m is the integrated stability correction function. Thus, the wakes of individual trees in typical forests persist up to about twice the canopy height, which corresponds to common estimates of the roughness sublayer height (Raupach et al., 1991). For a given reference height, the averaging length scale of a flux footprint is usually greater than the perturbation length scale of the dispersive flux (λ) indicated by (39) or (40) (Mahrt, 1996). Thus, if the flux footprint satisfies the representativeness criterion (36), it may be concluded that

the footprint average also covers a sufficient average of the dispersive flux to be spatially representative and satisfy (36) for the dispersive terms in (38).

The second and third terms on the RHS of (38) are the mean advective transport divergence, averaged over the horizontal domain. The relationship between these terms and carbon exchange measurements from a single tower are discussed in Lee (1998), Finnigan (1999), Baldocchi et al. (2000), and Paw U et al. (2000). Lee (1998) showed that vertical advection can be approximated by

$$\int_0^{z_m} \langle \bar{w} \rangle \frac{\partial \langle \bar{C} \rangle}{\partial z} \, dz \approx \langle \bar{w}_m \rangle (\langle \bar{C}(z_m) \rangle - [\bar{C}]) \qquad (41)$$

where $\bar{w}_m$ is the mean vertical velocity at the sensor height, z_m, and $[\bar{C}]$ is the volume averaged concentration. Lee (1998) compared several mechanisms that can give rise to a non-zero $\bar{w}_m$. Of these, only katabatic and anabatic circulations associated with terrain, and a potential systematic bias in daytime convection patterns over vegetation with low Bowen ratios appear to be strong enough to cause a significant vertical drift. These types of motion have horizontal scales on the order of 1–10 km or more and thus the vertical velocity is not expected to vary considerably over our reference spatial domain defined by the flux footprint in (38). Clearly, this type of inhomogeneity of the mean flow and its effect on biosphere–atmosphere exchange cannot be accounted for by a large enough footprint. However, Lee (1998) and Paw U et al. (2000) described methods to determine $\bar{w}_m$ experimentally and suggest procedures to account for the vertical advection term in the mass continuity equation.

The experimental determination of the concentration part on the RHS of (41) is closely associated with the measurement of the storage change term in (38) and is usually determined from $\bar{C}$-profile measurements between the forest floor and the reference height, z_m. As shown in Schmid (1994), the scalar concentration footprint is larger than the flux footprint in the same conditions, and thus the spatial averaging domain for $\langle \bar{C}(z_m) \rangle$ is larger than for $\langle F_C(z_m) \rangle$. Thus, if the footprint averaged flux, $\langle F_C(z_m) \rangle$, is deemed spatially representative of the forest and is satisfying (36), so is the footprint averaged concentration at the same height, unless the concentration footprint is so large that mesoscale landscape heterogeneity becomes important. However, both the volume average of C in (41) and the storage change term in (38) (first term on the RHS) involve concentration measurements from the reference height z_m all the way to the ground. If z_m refers to a measurement height above a forest canopy, and the lowest level of a measured C-profile is just a fraction of a meter above the forest floor, the footprint sizes along the profile are expected to vary by several orders of magnitude (note that, since the temporal development of the concentrations are considered here, and not a flux–gradient relationship, it is the concentration footprint and not the profile-flux footprint of Horst (1999) that comes to play here). If a footprint isopleth at any height is approximated by an ellipse, whose dimensions grow with height, the relevant averaging volume for the storage term in (38) resembles an inverted elliptical cone: the spatial reference at its base is considerably smaller than at the top. Two kinds of errors or biases can result from this. First, towers for above-canopy flux measurements are often located in gaps or small clearings of the canopy, to allow access to the tower and limit interference between trees and the tower or guy-wires. If C-profile measurements are conducted along such a tower, it must be expected that the lower portion of C-storage is affected by the emission, ventilation and mixing perturbations in the immediate vicinity of the tower. Second, in practice, the temporal integration of the storage term is commonly considered as the bulk increment between two discrete averaging periods on the order of 1/2–1 h. Non-stationarity at this time scale (e.g., a shift in flow direction, or change in stability) can cause the footprints of the two concentration measurements to be disparate. In this case, the bulk integration reflects the folding of spatial variability into a measured apparent temporal trend of storage change.

In summary, flux footprint estimates establish the spatial context of measured turbulent fluxes with reference to biosphere–atmosphere exchange. However, the spatial context of other measurable terms in the three-dimensional mass conservation equation is largely independent of the flux footprint and is likely to be disparate from it, rendering the spatial averaging operators for each term in (38) incongruous. The spatial consistency in estimates of NEE by the mass conservation equation can be evaluated by representativeness criteria, such as (36), for each term in the equation. Footprint considerations are inherently incapable of directly addressing contributions to the

mass budget due to spatial variations in the flow and turbulence fields (i.e., the advection and dispersive flux terms in (38)). Methods to evaluate and correct for such effects are discussed in Lee (1998), Finnigan (1999), Baldocchi et al. (2000) and Paw U et al. (2000), among others.

4. Future directions of footprint modeling applications

The dramatic increase of publications that address footprint modeling, applications or related issues of fetch and spatial representativeness for flux measurements in recent years demonstrates the growing need for practical footprint models. The development of a growing number of long-term trace gas exchange studies over complex forest canopies and in often topographically challenged terrain (such as those participating in the FLUXNET program) underlines the fact that the requirements for future footprint models are divergent: on the one hand, practical footprint models must be easy to use, if ever possible in the field, where the availability of computer resources (and time) is limited. The recent developments in analytical footprint models (Section 2.5) satisfy this need, but these models are limited to homogeneous surface layer similarity conditions. On the other hand, footprint models should produce realistic results in real-world situations for measurements over (or below) tall canopies, spatially heterogeneous turbulence, stability conditions from extremely stable to free-convective, and instationarity. Here, the backward Lagrangian models (Section 2.7) and the LES-based footprint studies (Section 2.8) provide first steps and hold promise of future progress, albeit at potentially extreme computational and resource expense. It seems that any one objective cannot be pursued without abandoning the other.

A form of compromise was suggested by Hsieh et al. (2000) and earlier by Schmid (1994): an "expensive" model is run over a range of input conditions, and the results are organized in non-dimensional groups and related to the input variables by regression analysis. In this way, a hybrid model is created in the form of an approximate or parameterized version of the full model. The advantages of such an approach are evident: the hybrid model can be expressed by a set of explicit algebraic equations, while some of the complexity and skill of the full model is retained through the regression. However, the pitfall of any approximation or parameterization is that its validity is strictly limited to the range of conditions over which it was developed.

With a view to the divergent demands on future footprint models, and from the perspective of the current state-of-the-art, a number of problems and desirable research directions for footprint modeling emerge:

- There is a general need for footprint model validation. Data for such validations could be provided by tracer release experiments where both concentrations and scalar fluxes are measured. A small number of suitable tracer experiments exist for dispersion in a homogeneous surface layer over short vegetation. No validation data are currently available for forest canopy footprint models. An alternative to tracer releases that can provide some insight is the further development of LES applications towards the simulation of realistic scenarios.
- Footprint models that are applicable to tall vegetation need to become more realistic. This objective requires a better understanding of the turbulence structure in forest canopies. LS models adapted to forest canopies are dependent on ad hoc assumptions about the profiles of turbulence statistics, and on local isotropy of small-scale turbulence, which are not strictly warranted. Important issues that hamper progress along these lines include experimental difficulties, spatial heterogeneity, clumpiness of the vegetation, and instationarity of canopy layer turbulence.
- The problem of horizontal inhomogeneity in the flow field needs to be addressed. Both backward Lagrangian models and LES-based footprint evaluations can cope with horizontal inhomogeneity in principle, but this needs to be demonstrated in practice. Forward Lagrangian models can handle horizontally inhomogeneous flow only at great computational expense. One challenge here is that the range of heterogeneous geometries is infinite. Generalizations tend to be either impossible or trivial.
- Forest edges or gaps are common within the "expected footprint" of many tower-based flux measurements. Their effect on the footprint is largely

unknown. Again, LES applications can provide guidance in principle, but the computational expense, and lack of turbulence data for validation are immense obstacles. The applicability of backward LS models in this context needs to be explored, but the lack of turbulence information is bound to remain a limiting factor.

- The influence of topography on flux footprints has been largely ignored to date. With many FLUXNET sites situated in topographically exposed or steep terrain, this issue is rapidly moving to the center.

This list of footprint modeling issues is by no means meant to be exhaustive. Most of the problems and challenges are interrelated and all of them are at the center of inquiry in the "new" micrometeorology of the real-world.

Acknowledgements

The author is indebted to Tom Horst, Natascha Kljun, Mathias Rotach, Hong-Bing Su, and John Wilson for many valuable comments and suggestions on the manuscript of this paper. The work of my graduate student Gabriella Villani, about the sensitivity of footprint predictions to discontinuities in the turbulence profiles, will be presented in a forthcoming paper. This work was supported by the National Institute of Global Environmental Change through the US Department of Energy (US-DOE Co-operative Agreement No. DE-FC03-90ER61010) and by a grant from the Terrestrial Carbon Processes program of US-DOE (through a subcontract from Harvard University). All opinions, findings, conclusions, and recommendations are those of the author and do not necessarily reflect the views of US-DOE.

References

Baldocchi, D., 1997. Flux footprints within and over forest canopies. Boundary-Lay. Meteorol. 85, 273–292.

Baldocchi, D., Finnigan, J., Wilson, K.T., Paw, U., Falge, E., 2000. On measuring net ecosystem carbon exchange over tall vegetation on complex terrain. Boundary-Lay. Meteorol. 96, 257–291.

Calder, K.L., 1952. Some recent British work on the problem of diffusion in the lower atmosphere. In: Proceedings of the US Technology Conference on Air Pollution, McGraw Hill, New York, pp. 787–792.

Cellier, P., Brunet, Y., 1992. Flux–gradient relationships above tall plant canopies. Agric. For. Meteorol. 58, 93–117.

Cionco, R.M., 1978. Analysis of canopy index values for various canopy densities. Boundary-Lay. Meteorol. 15, 81–93.

Claussen, M., 1989. Subgridscale fluxes and flux divergences in a neutrally stratified, horizontally homogeneous surface layer. Contr. Atmos. Phys. 62, 236–245.

Ehman, J.L., Schmid, H.P., Grimmond, C.S.B., Randolph, J.C., Hanson, P.J., Wayson, C.A., Cropley, F.D., 2002. An initial inter comparison of micrometeorological and ecological estimates of carbon sequestration in a mid-latitude deciduous forest. Glob. Change Biol. 8, 575–589.

Elliott, W.P., 1958. The growth of the atmospheric internal boundary layer. Trans. Amer. Geophys. Union 39, 1048–1054.

Finn, D., Lamb, B., Leclerc, M.Y., Horst, T.W., 1996. Experimental evaluation of analytical and Lagrangian surface-layer flux footprint models. Boundary-Lay. Meteorol. 80, 283–308.

Finnigan, J., 1999. A comment on the paper by Lee (1998): on micrometeorological observations of surface–air exchange over tall vegetation. Agric. For. Meteorol. 97, 55–64.

Finnigan, J., 2000. Turbulence in plant canopies. Annu. Rev. Fluid Mech. 32, 519–571.

Flesch, T.K., 1996. The footprint for flux measurements, from backward Lagrangian stochastic models. Boundary-Lay. Meteorol. 78, 399–404.

Flesch, T.K., Wilson, J.D., Yee, E., 1995. Backward-time Lagrangian stochastic dispersion models and their application to estimate gaseous emissions. J. Appl. Meteorol. 34, 1320–1332.

Garratt, J.R., 1990. The internal boundary layer. Boundary-Lay. Meteorol. 50, 171–203.

Gash, J.H.C., 1986. A note on estimating the effect of a limited fetch on micrometeorological evaporation measurements. Boundary-Lay. Meteorol. 35, 409–414.

Goulden, M.L., Munger, J.W., Fan, S.-M., Daube, B.C., Wofsy, S.C., 1996. Measurements of carbon sequestration by long-term eddy covariance: methods and a critical evaluation of accuracy. Glob. Change Biol. 2, 169–182.

Gryning, S.E., van Ulden, A.A.M., Larsen, S., 1983. Dispersion from a continuous ground level source investigated by a K model. Quart. J. Roy. Meteorol. Soc. 109, 355–364.

Gryning, S.E., van Ulden, A.A.M., Irwin, J.S., Sievertsen, D., 1987. Applied dispersion modelling based on meteorological scaling parameters. Atmos. Environ. 21, 79–89.

Hadfield, M.G., 1994. Passive scalar diffusion from surface sources in the convective boundary-layer. Boundary-Lay. Meteorol. 69, 417–448.

Haenel, H.D., Grünhage, L., 1999. Footprint analysis: a closed analytical solution based on height-dependent profiles of wind speed and eddy viscosity. Boundary-Lay. Meteorol. 93, 395–409.

Højstrup, J., 1981. A simple model for the adjustment of velocity spectra in unstable conditions downstream of an abrupt change in roughness and heat flux. Boundary-Lay. Meteorol. 21, 341–356.

Holtslag, A.A.M., Nieuwstadt, F.T.M., 1986. Scaling the atmospheric boundary layer. Boundary-Lay. Meteorol. 36, 201–209.

Horst, T.W., 1979. Lagrangian similarity modeling of vertical diffusion from a ground-level source. J. Appl. Meteorol. 12, 797–802.

Horst, T.W., 1999. The footprint for estimation of atmosphere-surface exchange fluxes by profile techniques. Boundary-Lay. Meteorol. 90, 171–188.

Horst, T.W., Weil, J.C., 1992. Footprint estimation for scalar flux measurements in the atmospheric surface-layer. Boundary-Lay. Meteorol. 59, 279–296.

Horst, T.W., Weil, J.C., 1994. How far is far enough—the fetch requirements for micrometeorological measurement of surface fluxes. J. Atmos. Oceanic Technol. 11, 1018–1025.

Horst, T.W., Weil, J.C., 1995. Corrigenda: How far is far enough—the fetch requirements for micrometeorological measurement of surface fluxes. J. Atmos. Oceanic Technol. 12, 447.

Horst, T.W., 2001. Comments on "Footprint analysis: a closed analytical solution based on height-dependent profiles of wind speed and eddy viscosity", by Haenel and Grünhage (1999). Boundary-Lay. Meteorol. 101. 435–447.

Hsieh, C.I., Katul, G.G., Schieldge, J., Sigmon, J.T., Knoerr, K.K., 1997. The Lagrangian stochastic model for fetch and latent heat flux estimation above uniform and non-uniform terrain. Water Resour. Res. 33, 427–438.

Hsieh, C.I., Katul, G., Chi, T., 2000. An approximate analytical model for footprint estimation of scaler fluxes in thermally stratified atmospheric flows. Adv. Water Resour. 23, 765–772.

Kaimal, J.C., Finnigan, J.J., 1994. Atmospheric Boundary Layer Flows: their Structure and Measurement. Oxford University Press, New York, 289 pp.

Kljun, N., Rotach, M.W., Schmid, H.P., 1999. Allocation of surface sources for elevated trace gas fluxes using "backward trajectory"-simulations. In: Proceedings of the 13th Symposium on Boundary Layers and Turbulence. Preprints. American Meteorological Society, Boston, p. J4.7.

Kljun, N., Rotach, M.W, Schmid, H.P., 2000a. A Lagrangian footprint model for stratifications ranging from stable to convective. In: Proceedings of the 14th Symposium on Boundary Layers and Turbulence. Preprints. American Meteorological Society, Boston, p. 4.15.

Kljun, N., de Haan, P., Rotach, M.W., Schmid, H.P., 2000b. Footprint determination in stable to convective stratification using an inverse 3D Lagrangian particle model. In: Proceedings of the 24th Conference on Agricultural and Forest Meteorology. Preprints. American Meteorological Society, Boston, p. 8.3.

Kljun, N., Rotach, M.W., Schmid, H.P., 2002. A 3-D backward Lagrangian footprint model for a wide range of boundary layer stratifications. Boundary-Lay. Meteorol. 103, 205–226.

Kormann, R., Meixner, F.X., 2001. An analytic footprint model for neutral stratification. Boundary-Lay. Meteorol. 99, 207–224.

Kurbanmuradov, O., Sabelfeld, K.K., 2001. Lagrangian stochastic models for turbulent dispersion in the atmospheric boundary layer. Boundary-Lay. Meteorol. 97, 191–218.

Leclerc, M.Y., Thurtell, G.W., 1990. Footprint prediction of scalar fluxes using a Markovian analysis. Boundary-Lay. Meteorol. 52, 247–258.

Leclerc, M.Y., Shen, S.H., Lamb, B., 1997. Observations and large-eddy simulation modeling of footprints in the lower convective boundary layer. J. Geophys. Res. Atmos. 102, 9323–9334.

Lee, X., 1998. On micrometeorological observations of surface-air exchange over tall vegetation. Agric. For. Meteorol. 91, 39–49.

Legg, B.J., Raupach, M.R., 1982. Markov-chain simulation of particle dispersion in inhomogeneous flows: the mean drift velocity induced by a gradient in Eulerian velocity variance. Boundary-Lay, Meteorol. 24, 3–13.

Leonard, A., 1974. Energy cascade in large-eddy simulations of turbulent fluid flows. Adv. Geophys. A 18, 237–248.

Lin, J.S., Hildemann, L.M., 1996. Analytical solutions of the atmospheric diffusion equation with multiple sources and height-dependent wind speed and eddy diffusivities. Atmos. Environ. 30, 239–254.

Luhar, A.K., Britter, R., 1989. Random walk model studies for dispersion in inhomogeneous turbulence in convective boundary layers. Atmos. Environ. 23, 1911–1924.

Luhar, A.K., Rao, K.S., 1994. Source footprint analysis for scalar fluxes measured in flows over inhomogeneous surface. In: Gryning, S.E., Millan, M.M. (Eds.), Air Pollution Modelling and its Application, Vol. X. Plenum Press, New York, pp. 315–323.

Mahrt, L., 1987. Grid averaged surface fluxes. Mon. Weath. Rev. 115, 1550–1560.

Mahrt, L., 1996. The bulk aerodynamic formula over heterogeneous surfaces. Boundary-Lay. Meteorol. 78, 87–119.

Mason, P.J., 1994. Large-eddy simulation: a critical review of the technique. Quart. J. Roy. Meteorol. Soc. 120, 1–26.

Moeng, C.-H., 1984. A large-eddy simulation model for the study of planetary boundary layer turbulence. J. Atmos. Sci. 41, 2052–2061.

Nieuwstadt, F.T.M., de Valk, A., 1987. A large-eddy simulation of buoyant and non-buoyant plume dispersion in the atmospheric boundary layer. Atmos. Environ. 12, 1305–1311.

Panofsky, H.A., 1973. Tower micrometeorology. In: Haugen, D.H. (Ed.), Workshop on Micrometeorology. American Meteorological Society, Boston, pp. 151–176.

Pasquill, F., 1972. Some aspects of boundary layer description. Quart. J. Roy. Meteorol. Soc. 98, 469–494.

Pasquill, F., Smith, F.B., 1983. Atmospheric Diffusion, 3rd Edition. Wiley, New York, 437 pp.

Paw U, K.T., Baldocchi, D.D., Meyers, T.P., Wilson, K.B., 2000. Correction of eddy-covariance measurements incorporating both advective effects and density fluxes. Boundary-Lay. Meteorol. 97, 487–511.

Perrier, A., Tuzet, A., 1991. Land surface processes: description, theoretical approaches, and physical laws underlying their measurement. In: Schmugge, T.J., André, J.C. (Eds.), Land Surface Evaporation—Measurement and Parameterization. Springer, New York, pp. 145–155.

Peterson, E.W., 1969. Modification of mean flow and turbulent energy by a change in surface roughness under conditions of neutral stability. Quart. J. Roy. Meteorol. Soc. 95, 561–575.

Rannik, Ü., Aubinet, M., Kurbanmuradov, O., Sabelfeld, K.K., Markkanen, T., Vesala, T., 2000. Footprint analysis for

measurements over a heterogeneous forest. Boundary-Lay. Meteorol. 97, 137–166.

Rao, K.S., 1975. Effect of thermal stratification on the growth of the internal boundary-layer. Boundary-Lay. Meteorol. 8, 227–234.

Raupach, M.R., 1988. Canopy transport processes. In: Steffen, W.L., Denmead, O.T. (Eds.), Flow and Transport in the Natural Environment: Advances and Application. Springer, Berlin, pp. 95–127.

Raupach, M.R., 1989. Applying Lagrangian fluid mechanics to infer scalar source distributions from concentration profiles in plant canopies. Agric. For. Meteorol. 47, 85–108.

Raupach, M.R., Antonia, R.A., Rajagopalan, S., 1991. Rough wall turbulent boundary layers. Appl. Mech. Rev. 44, 1–25.

Reynolds, A.M., 1998. A two-dimensional Lagrangian stochastic dispersion model for convective boundary layers with wind shear. Boundary-Lay. Meteorol. 86, 345–352.

Rodean, H., 1996. Stochastic Lagrangian models of turbulent diffusion. Meteorological Monographs, Vol. 26, No. 48. American Meteorological Society, Boston, 84 pp.

Rotach, M.W., Gryning, S.-E., Tassone, C., 1996. A two-dimensional stochastic dispersion model for daytime conditions. Quart. J. Roy. Meteorol. Soc. 122, 367–389.

Sawford, B.L., Guest, F.M., 1987. Lagrangian stochastic analysis of flux gradient relationships in the convective boundary layer. J. Atmos. Sci. 44, 1152–1165.

Schlichting, H., 1968. Boundary Layer Theory, 4th Edition. McGraw Hill, New York, 747 pp.

Schmid, H.P., 1988. Spatial scales of sensible heat flux variability: representativeness of flux measurements and surface layer structure over suburban terrain. Ph.D. Thesis. The University of British Columbia, Vancouver, Canada, 299 pp.

Schmid, H.P., 1994. Source areas for scalars and scalar fluxes. Boundary-Lay. Meteorol. 67, 293–318.

Schmid, H.P., 1997. Experimental design for flux measurements: matching the scales of observations and fluxes. Agric. For. Meteorol. 87, 179–200.

Schmid, H.P., Lloyd, C.R., 1999. Location bias of flux measurements over inhomogeneous areas. Agric. For. Meteorol. 93, 195–209.

Schmid, H.P., Oke, T.R., 1988. Estimating the source area of a turbulent flux measurement over a patchy Surface. In: Proceedings of the Eighth Symposium on Turbulence and Diffusion. Preprints. American Meteorological Society, Boston, MA, pp. 123–126.

Schmid, H.P., Oke, T.R., 1990. A model to estimate the source area contributing to turbulent exchange in the surface-layer over patchy terrain. Quart. J. Roy. Meteorol. Soc. 116, 965–988.

Schmid, H.P., Cleugh, H.A., Grimmond, C.S.B., Oke, T.R., 1991. Spatial variability of energy fluxes in suburban terrain. Boundary-Lay. Meteorol. 54, 249–276.

Schmid, H.P., Grimmond, C.S.B., Cropley, F., Offerle, B., Su, H.-B., 2000. Measurements of CO_2 and Energy Fluxes over a Mixed Hardwood Forest in the Midwestern United States. Agric. For. Meteorol. 103, 355–373.

Schuepp, P.H., Leclerc, M.Y., Macpherson, J.I., Desjardins, R.L., 1990. Footprint prediction of scalar fluxes from analytical solutions of the diffusion equation. Boundary-Lay. Meteorol. 50, 353–373.

Smith, F.B., 1957. The diffusion of smoke from a continuous elevated point source into a turbulent atmosphere. J. Fluid Mech. 2, 49.

Stannard, D.I., 1997. A theoretically based determination of Bowen ratio fetch requirements. Boundary-Lay. Meteorol. 83, 375–406.

Su, H.-B., Leclerc, M.Y., 1998. Large-eddy simulation of trace gas footprints from infinite crosswind line sources inside a forest canopy. In: Proceedings of the 23rd Conference on Agricultural and Forest Meteorology. Preprints. American Meteorological Society, Boston, MA, pp. 388–391.

Su, H.-B., Shaw, R.H., Paw U, K.T., Moeng, C.-H., P Sullivan, P., 1998. Turbulent statistics of neutrally stratified flow within and above a sparse forest from large-eddy simulation and field observations. Boundary-Lay. Meteorol. 88, 363–397.

Thomson, D.J., 1987. Criteria for the selection of stochastic models of particle trajectories in turbulent flow. J. Fluid Mech. 180, 529–556.

Uchijima, Z., Wright, J.L., 1964. An experimental study of air flow in a corn plant air layer. Bull. Natl. Inst. Agric. Sci. Jpn. A 11, 19–44.

van Dop, H., Nieuwstadt, F.T.M., Hunt, J.C.R., 1985. Random walk models for particle displacements in inhomogeneous unsteady turbulent flows. Phys. Fluids 28, 1639–1653.

van Ulden, A.P., 1978. Simple estimates for vertical diffusion from sources near the ground. Atmos. Environ. 12, 2125–2129.

Weil, J.C., 1990. A diagnosis of the asymmetry in top-down and bottom-up diffusion using a Lagrangian stochastic model. J. Atmos. Sci. 47, 501–515.

Weil, J.C., Horst, T.W., 1992. Footprint estimates for atmospheric flux measurements in the convective boundary layer. In: Schwartz, S.E., Slinn, W.G.N. (Eds.), Precipitation Scavenging and Atmosphere–Surface Exchange, Vol. 2. Hemisphere, Washington, DC, pp. 717–728.

Willis, G.E., Deardorff, J.W., 1976. On the use of Taylor's translation hypothesis for diffusion in the mixed layer. Quart. J. Roy. Meteorol. Soc. 102, 817–822.

Wilson, J.D., Flesch, K.T., 1993. Flow boundaries in random-flight dispersion models: enforcing the well-mixed condition. J. Appl. Meteorol. 32, 1695–1707.

Wilson, J.D., Sawford, B.L., 1996. Review of Lagrangian stochastic models for trajectories in the turbulent atmosphere. Boundary-Lay. Meteorol. 78, 191–210.

Wilson, J.D., Swaters, G.E., 1991. The source area influencing a measurement in the planetary boundary-layer—the footprint and the distribution of contact distance. Boundary-Lay. Meteorol. 55, 25–46.